Hindawi
Evidence-Based Complementary and Alternative Medicine
Volume 2022, Article ID 1322751, 22 pages
https://doi.org/10.1155/2022/1322751

Research Article

Chemical Characterization and Metabolic Profiling of the Compounds in the Chinese Herbal Formula Li Chang Decoction by UPLC-QTOF/MS

Baofu Lin, Shaoju Guo, Xinxin Hong, Xiaoyan Jiang, Haiwen Li, Jingwei Li, Linglong Guo, Mianli Li, Jianping Chen, Bin Huang, and Yifei Xu

Shenzhen Traditional Chinese Medicine Hospital,
The Fourth Clinical Medical College of Guangzhou University of Chinese Medicine, Shenzhen 518033, China

Correspondence should be addressed to Bin Huang; sztcmhuangbin@163.com and Yifei Xu; xyf2995@gzucm.edu.cn

Received 16 February 2022; Revised 20 March 2022; Accepted 30 March 2022; Published 13 April 2022

Academic Editor: Maria Grazia Ferraro

Background. Li Chang decoction (LCD), a Chinese medicine formula, is commonly used to treat ulcerative colitis (UC) in clinics. *Purpose*. This study aimed to identify the major components in LCD and its prototype and metabolic components in rat biological samples. *Methods*. The chemical constituents in LCD were identified by establishing a reliable ultra-performance liquid chromatography coupled with quadrupole time-of-flight tandem mass spectrometry (UPLC-QTOF/MS) method. Afterwards, the rats were orally administered with LCD, and the biological samples (plasma, urine, and feces) were collected for further analyzing the effective compounds in the treatment of UC. *Result*. A total of 104 compounds were discriminated in LCD, including 26 flavonoids, 20 organic acids, 20 saponins, 8 amino acids, 5 oligosaccharides, 5 tannins, 3 lignans, 2 alkaloids, and 15 others (nucleosides, glycosides, esters, etc.). About 50 prototype and 94 metabolic components of LCD were identified in biological samples. In total, 29 prototype components and 22 metabolic types were detected in plasma. About 27 prototypes and 96 metabolites were discriminated in urine, and 34 prototypes and 18 metabolites were identified in feces. *Conclusion*. The flavonoids, organic acids, and saponins were the major compounds of LCD, and this study promotes the further pharmacokinetic and pharmacological evaluation of LCD.

1. Introduction

Traditional Chinese medicine (TCM) attracts more attention in the world since it possesses reliable therapeutic efficacy in some complex diseases, especially chronic illness [1]. The chemical composition of Chinese herbal compound is complex, and the composition of the multi-Chinese medicine is crossed, summarized as "multitarget and multicomponent," which is the feature of TCM [2, 3]. This characteristic promotes the curative effect and reduces toxicity; however, it brings enormous challenge to figure out the effective components and mechanism for the therapeutic effect [4].

Li Chang decoction (LCD), a Chinese compound prepared from twelve Chinese medicine including Codonopsis Radix (CR), Notoginseng Radix et Rhizoma (NRR), Bletillae Rhizoma (BR), Sophorae Flos (SF), Glycyrrhizae Radix et Rhizoma (GRR), Cynanchi Paniculati Radix et Rhizoma (CPRR), Typhae Pollen (TP), Chebulae Fructus (CF), Atractylodis Macrocephalae Rhizoma (AMR), Ailanthi Cortex (AC), Coicis Semen (CS), and Halloysitum Rubrum (HR), has been commonly used to treat ulcerative colitis (UC) in clinics for over 20 years(Figure 1). UC is a chronic disease of inflammatory bowel diseases, which seriously impact the life quality of patients, and is sometimes life-threatening. LCD remarkably reduces the symptoms and recurrence rate of UC in clinical [5]. Although some of the major ingredients such as the polysaccharides from CR and AMR and rutin from SF have been proved effective in the treatment of UC, the effective components of LCD are still controversial and unclear [6–8]. Therefore, the systematic

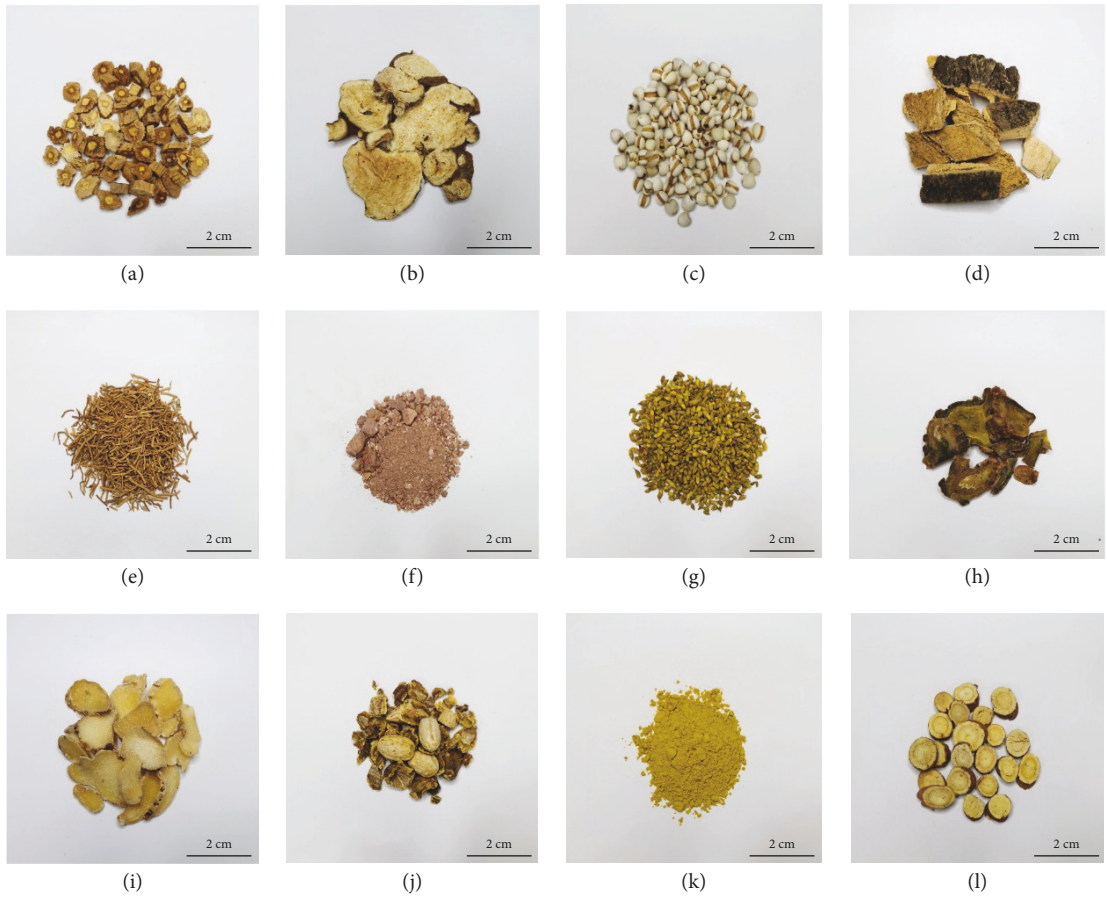

Figure 1: Decoction samples of 12 Chinese herbal medicines in LCD. (a) Codonopsis Radix; (b) Atractylodis Macrocephalae Rhizoma; (c) Coicis Semen; (d) Ailanthi Cortex; (e) Cynanchi Paniculati Radix et Rhizoma; (f) Halloysitum Rubrum; (g) Sophorae Flos; (h) Notoginseng Radix et Rhizoma; (i) Bletillae Rhizoma; (j) Chebulae Fructus; (k) Typhae Pollen; (l) Glycyrrhizae Radix et Rhizoma.

research on the effective component and metabolite profiling of LCD is an urgent need.

Ultra-performance liquid chromatography coupled with quadrupole time-of-flight tandem mass spectrometry (UPLC-QTOF/MS) provides a rapid and reliable method to identify the component of natural medicine, which promotes the development of natural medicine component analysis and new drug discovery [9, 10]. Herein, we recruited an UPLC-QTOF/MS method to profile the effective components of LCD, and the unknown components were classified and assigned based on the fragmentation patterns and diagnostic ions of different structural types of components. According to the component characterization result of LCD *in vitro*, the prototypes in plasma, urine, and feces were further analyzed based on the similarity of mass spectrometry behavior (accurate molecular weight and secondary fragments) and chromatographic behavior (retention time). Metabolites were matched *e* mass defect filtering (MDF) caused by biotransformation and were further confirmed by MS/MS spectrum analysis.

2. Material and Methods

2.1. Chemicals and Drugs. LCD was prepared by the Pharmaceutical Department, Shenzhen Traditional Chinese Medicine Hospital. The Chinese medicine including Codonopsis Radix (Lot: 190505101, root of *Codonopsis pilosula* (Franch.) Nannf.), Atractylodis Macrocephalae Rhizoma (Lot: 1904001, rhizoma of *Atractylodes macrocephala* Koidz.), Chebulae Fructus (Lot: 181203361, fructus of *Terminalia chebula* Retz.), Halloysitum Rubrum (Lot: 190300991), Sophorae Flos (Lot: 190504381, flos of *Sophora japonica* L.), Typhae Pollen (Lot: 190401, pollen of *Typha angustifolia* L.), Ailanthi Cortex (Lot: 181001, cortex of *Ailanthus altissima* (Mill.) Swingle), Bletillae Rhizoma (Lot: HX19K01, rhizoma of *Bletilla striata* (Thunb.) Reichb. f), Coicis Semen (Lot: 1905002, semen of *Coix lacryma-jobi* L. var. *ma-yuen* (roman) Stapf), Notoginseng Radix et Rhizoma (Lot: 190401411, radix and rhizoma of *Panax notoginseng* (Burk.) F. H. Chen), Cynanchi Paniculati Radix et Rhizoma (Lot: 190403711, radix and rhizoma of *Cynanchum paniculatum* (Bge.) Kitag.), and Glycyrrhizae Radix et Rhizoma (Lot: 1905001, radix and rhizoma of *Glycyrrhiza uralensis* Fisch.) was purchased from Kangmei Pharmaceutical Co., Ltd (Puning, China). Trigonelline, chebulic acid, gallic acid, 6,7-dihydroxycoumarin, corilagin, typhaneoside, rutin, hyperoside, liquiritin, nicotiflorin, lobetyolin, ginsenoside Re, ginsenoside Rg1, quercetin, ginsenoside Rb1, naringenin, 20S-ginsenoside Rh1, isorhamnetin, ginsenoside Rd, and glycyrrhizic acid, a total of 20 reference standards, were purchased from Chengdu Alfa

Biotechnology Co., Ltd. The purity of each compound was more than 98% determined by the HPLC analysis. Methanol was of HPLC grade. Ultrapure water was obtained by the filtration of distilled water using a Milli-Q system (Millipore, USA). LC-MS grade acetonitrile was purchased from Fisher Scientific (Fair Lawn, New Jersey, USA), and LC-MS grade formic acid was purchased from Sigma-Aldrich (St, Missouri, USA).

2.2. Animal. Male Sprague-Dawley rats (300 ± 20 g) were obtained from the Medical Experimental Animal Center of Guangzhou University of Chinese Medicine, China. Rats were housed in specified pathogen-free conditions (23 ± 2°C) under a 12-h light/12-h dark cycle and given free access to food and water. The protocols were approved by the Animal Experimental Ethics Committee of Guangzhou University of Chinese Medicine (Guangzhou, China).

2.3. LCD Preparation. The Medicine Codonopsis Radix, Atractylodis Macrocephalae Rhizoma, Chebulae Fructus, Halloysitum Rubrum, Sophorae Flos, Typhae Pollen, Ailanthi Cortex, Bletillae Rhizoma, Coicis Semen, Notoginseng Radix et Rhizoma, Cynanchi Paniculati Radix et Rhizoma, and Glycyrrhizae Radix et Rhizoma were weighed and mixed at a ratio of 6 : 3:3 : 6:3 : 3:6 : 3:6 : 2:6 : 2. The total weight of LCD is 245g, and the mixture was extracted twice by boiling in distilled water, and eight times distilled water (1960 ml) (w/v) was used to boil for 40 min in the first time, which changes to four times distilled water (980 ml) (w/v) in the second time. The two extracts were merged and centrifuged at 3,000 rpm, for 5 min to exclude dregs, and the supernatant was concentrated to 3.185 g/ml under reduced pressure at 55°C.

2.4. Rat Treatment and Sample Collection. The dose of LCD used in this experiment is 22.05 g/kg, which is the biological equivalent dose of humans. Three rats were fasted for 12 h with free access to drinking water, and then, the rats were orally administered with LCD. LCD was diluted to 2.205 g/ml with distilled water before giving to rat. Then, the blood samples were collected in the heparin anticoagulant tube through retro-orbital plexus at 0.25, 0.5, 1, 2, 4, 6, 8, 10, and 12 h. The plasma samples were obtained by centrifugation at 3000 rpm for 10 min. Samples of the same point were combined and stored at −80°C until use. Feces and urine samples were collected during 0–12 h.

2.5. Biological Sample Preparation. For the plasma sample, about 200 μl plasma was mixed with 600 μl acetonitrile (containing 0.2% methanoic acid). After vortexing for 2 min, the samples were centrifuged at 13000 rpm, 4°C, 10 min. Then, 400 μl supernatant was removed, dried under nitrogen gas, and redissolved in 100 μl acetonitrile (50%). Finally, the samples were centrifuged at 13000 rpm, 4°C, 10 min, and a 2 μl aliquot was injected into UPLC-QTOF-MS.

For the fecal sample, about 300 mg of feces was weighed and mixed with 1 ml methanol. After the addition of magnetic beads, the samples were homogenized using tissue grinders (Shanghai Jingxin, Shanghai, China) and centrifuged at 13000 rpm, 4°C, 10 min. About 200 μl supernatant was removed, dried under nitrogen gas, and redissolved in 200 μl acetonitrile (50%). Finally, the samples were centrifuged at 13000 rpm, 4°C, 10 min, and a 2 μl aliquot was injected into UPLC-QTOF-MS.

For the urine sample, the mixed urine was centrifuged at 4000 rpm for 10 min, and 1 ml supernatant was loaded on pre-activated Sep-Pak Vac C18 columns (3 cc, 500 mg, Waters, Ireland). After washing with 1 ml ultrapure water and eluting with 1 ml methanol, the elution was collected and centrifuged at 13000 rpm, 4°C, 10 min. About 400 μl supernatant was transferred and dried under nitrogen gas. The residues were redissolved in 400 μl acetonitrile (50%). Finally, the samples were centrifuged at 13000 rpm, 4°C, 10 min, and a 2 μl aliquot was injected into UPLC-QTOF-MS.

2.6. UPLC-QTOF-MS Analysis Condition. The separation equipment for this assay was Sciex Exion LC, and the chromatographic column was Waters Acquity HSS T3 (2.1 × 150 mm, 1.7 μm). The temperature was set at 35°C, and the flow rate was 0.3 ml/min. The mobile phases were 0.1% formic acid in water (A) and acetonitrile (B), with the optimized gradient as follows: 0–5 min from 3% B to 8% B, 5–11 min from 8% B to 30% B, 11–20 min from 30% B to 80% B, 20–21 min from 80% B to 95% B, 21–25 min was maintained at 95% B, and then back to the initial ratio and re-equilibration for 7 min.

The 5600 QTOF mass spectrometer (AB Sciex, Foster City, CA, USA) equipped with an ESI ion source was operated in positive and negative modes, and the mass range was *m/z* of 100–1250. The details of mass spectrometry conditions were summarized as follows: gas 1 and gas 2, 45 psi; curtain gas, 35 psi; heat block temperature, 500°C; ion spray voltage, −4.5 kV in negative mode and 5.5 kV in positive; declustering potential, 50V; collision energy, ±35 V; and the collision energy spread (CES), ±15 V. Sciex OS 1.6.1 was the basal data processing platform, and MetabolitePilot 2.0.4 software was applied for further metabolite fishing.

3. Results and Discussion

3.1. Characterization of Chemical Compounds in LCD. The base peak chromatograms of LCD in negative and positive ion modes are shown in Figure 2. A total of 104 chemical components, including 20 saponins, 26 flavonoids, 5 tannins, 20 organic acids, 8 amino acids, 2 alkaloids, 5 oligosaccharides, and 3 lignans, were identified or tentatively characterized by UPLC-QTOF-MS. As the result of chemical composition classification is summarized in Table 1, CR mainly contained alkaloid compounds and oligosaccharides, while NRR was characterized by saponins. Besides, the major constituents of SF were flavonoids. GRR contains saponins and flavonoids, and CPRR was as characterized by the C21 type steroidal saponins. The characteristic ingredients of TP were flavonoids and organic acids. CF was characterized by the component of tannins; AMR contains organic acids and esters.

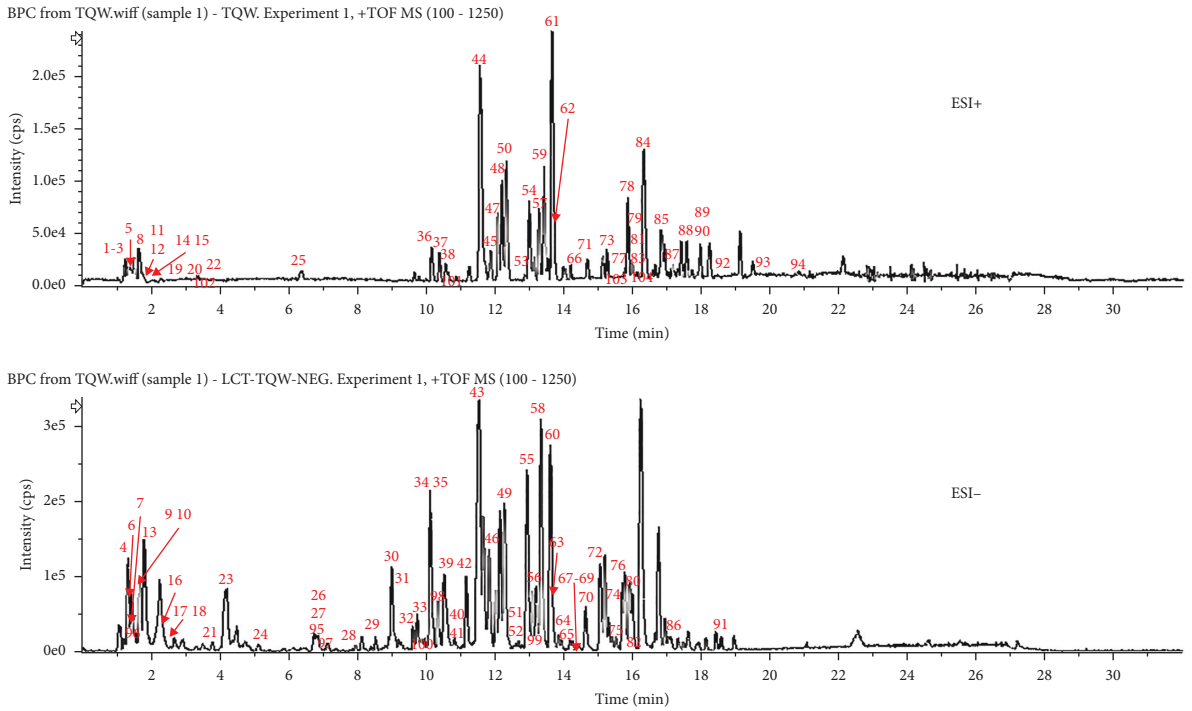

Figure 2: Base peak chromatogram (BPC) of LCD.

Table 1: Chemical component of LCD.

	Alkaloid	Amino acid	Oligosaccharides	Saponins	Lignans	Flavonoids	Organic acids	Tannins	Others (Nucleosides, glycosides, esters, etc.)	Total
CR	2	4	5	—	—	—	—	—	6 (3)	17
NRR	—	—	—	9	—	—	—	—	—	9
BR	—	—	—	—	3	—	1	—	1	5
SF	—	1	—	2	—	8 (3)	—	—	2	13
GRR	—	—	—	8	—	14	—	—	1	23
CPRR	—	—	—	1	—	—	—	—	—	1
TP	—	3	—	—	—	5 (2)	6 (2)	—	2 (1)	16
CF	—	—	—	—	—	—	5 (1)	5	1	11
AMR	—	—	—	—	—	—	1	—	2 (1)	3
CS	—	—	—	—	—	3 (3)	10 (4)	—	2 (1)	15
AC	—	—	—	—	—	2 (2)	1 (1)	—	1	4
Total	2	8	5	20	3	26	20	5	15	104

The number in the brackets was the repeat compounds.

Generally, the characteristic components of AC were triterpenes, and the CS was characterized by lipids. However, both chemical categories were difficult to extract by water so that only flavonoids and organic acids in AC and CS were still detected and identified. Figure 3 draws the part of representative structures of each medicine.

3.2. Fragmentation Mechanisms of Medicine Representative Structures

3.2.1. Codonopsis Radix-Derived Compounds. A total of 17 compounds were identified in CR. Among them, saccharides (**P4** fructose, **P6** sucrose, **P7** raffinose, **P8** stachyose, and **P14** verbascose) and alkaloids (**P5** trigonelline and **P25** codonopsine) were characteristic components [11, 12]. Saccharides showed $[M\text{-}H]^-$ in the negative ion mode and $[M+NH_4]^+/[M+Na]^+$in the positive ion mode. The successive neutral loss of hexose (−162 Da) and H_2O (−18 Da) was used for identification. The typical fragmentation pattern of **P14** verbascose is drawn in Figure 4(a). Alkaloid **P5** trigonelline produced a $[M+H]^+$ ion at *m/z* of 138.0546 and had fragment ions at *m/z* of 94, 92, and 78, which correspond to $[M\text{-}CO_2+H]^+$, $C_6H_6N^+$, and $C_5H_4N^+$, respectively. P25 codonopsine showed $[M+H]^+$ ion at *m/z* of 268.1546, and

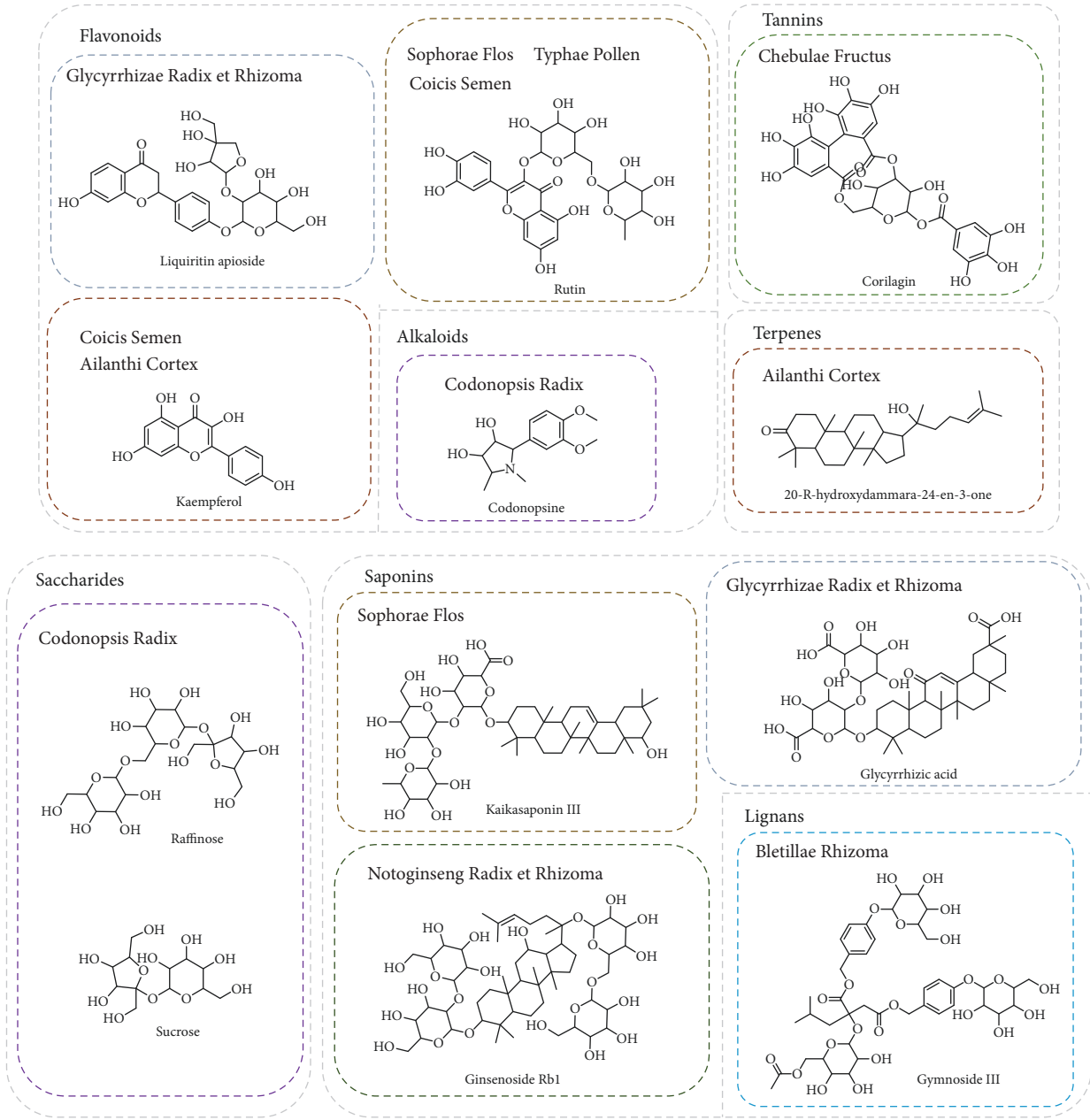

Figure 3: Continued.

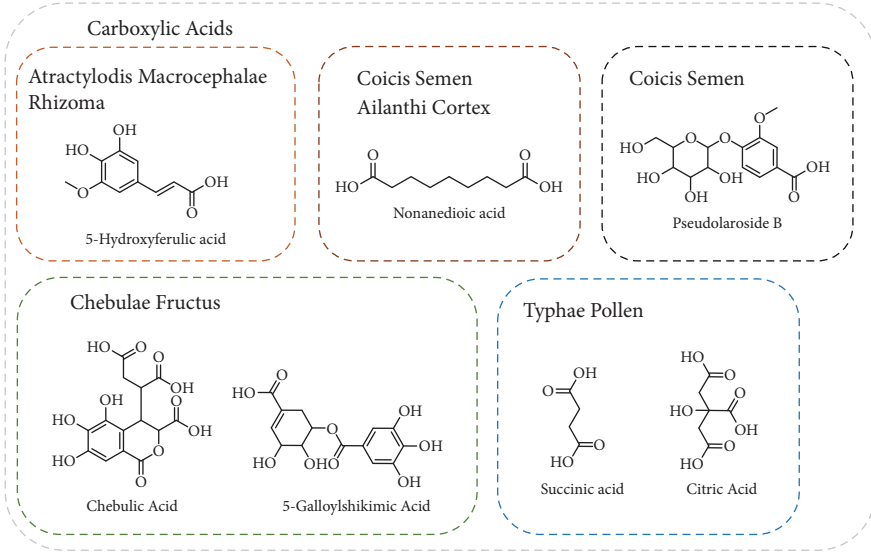

Figure 3: Representative structures of each medicine of LCD.

the fragment ions at *m/z* of 161, 88, and 58 were produced by penta-heterocycle cracking. The typical fragmentation pathways of **P5** trigonelline are drawn in Figure 4(b).

3.2.2. Notoginseng Radix et Rhizoma-Derived Compounds. About 9 compounds were identified in Notoginseng Radix et Rhizoma, and all of the compounds were triterpenoid saponins (**P55** notoginsenoside E, **P58** ginsenoside Re, **P59** ginsenoside Rg1, **P72** ginsenoside Rb1, **P74** notoginsenoside R2, **P76** 20s-ginsenoside Rh1, **P77** ginsenoside Rh4/Rk3, **P82** ginsenoside Rd, and **P91** ginsenoside F2) [13–15].

The neutral loss of Glc (162 Da) and Rha (146 Da) was characteristically appeared in saponin compounds. **P59** ginsenoside Rg1 is taken as example, and it had the $[M + HCOO]^-$ ion at *m/z* of 845.4899 and $[M + H]^+$ ion at *m/z* of 801.4983. The characteristic product ions at *m/z* of 621 $[M\text{-}Glc\text{-}H_2O]^+$, 603 $[M\text{-}Glc\text{-}2H_2O]^+$, 441 $[M\text{-}2Glc\text{-}2H_2O]^+$, 423 $[M\text{-}2Glc\text{-}3H_2O]^+$, and 405 $[M\text{-}2Glc\text{-}4H_2O]^+$ were observed. The typical fragmentation pathways of **P59** ginsenoside Rg1 are drawn in Figure 4(c).

3.2.3. Bletillae Rhizoma-Derived Compounds. A total of 5 characteristic compounds were detected in Bletillae Rhizoma. **P47** dactylorhin A [16], **P56** gymnoside III, and **P61** militarine [17] were structurally similar to that contained two molecules of gastrodin (P22). Neutral loss of Glc (162 Da), H_2O (18 Da), and gastrodin (268 Da) was used for identification. **P47** dactylorhin A showed the $[M - H]^-$ ion at *m/z* of 887.3181 and $[M + NH_4]^+$ ion at *m/z* of 906.3601, while it had characteristic fragment ion at $[M\text{-}Glc\text{-}H_2O\text{–}H]^-$ at *m/z* of 707, $[M\text{-gastrodin-H}]^-$ at *m/z* of 619, $[M\text{-gastrodin-Glc-}H_2O\text{–H}]^-$ at *m/z* of 439, $[M\text{-gastrodin-Glc} + H]^+$ at *m/z* of 459, $[gastrodin]^+$ at *m/z* of 269, and $[gastrodin\text{-Glc}]^+$ at *m/z* of 107. The typical fragmentation pathways of **P47** dactylorhin A are drawn in Figure 4(d).

3.2.4. Sophorae Flos-Derived Compounds. Thirteen compounds were isolated from Sophorae Flos [18–20], and more than half of them were flavonoids, or specifically flavonols (**P37** quercetin 3-O-glucosyl-rutinoside [21], **P39** manghaslin [22], **P43** rutin [23–25], **P45** isoquercitrin [26], **P48** nicotiflorin [27], **P50** narcissin [24, 28], **P70** quercetin [23, 29, 30], and **P79** isorhamnetin [22]). In negative mode, flavonoid glycosides were trend to neutral loss of glycosides. In addition, neutral losses of CH3 (15 Da), CO (28 Da), and RDA cracking could also be observed. **P43** rutin was a vital constituent of Sophorae Flos. It had the $[M + H]^+$ ion at *m/z* of 611.1607 and gave characteristic fragment ions at *m/z* of 465 and 303 by successive loss of Glc (162 Da) and Rha (146 Da). The typical fragmentation pathways of **P43** rutin are drawn in Figure 4(e).

3.2.5. Glycyrrhizae Radix et Rhizoma-Derived Compounds. A total of 23 compounds were discriminated in Glycyrrhizae Radix et Rhizoma, and 14 of them were flavonoids (**P44** licuraside/liquiritin apioside, **P46** liquiritin, **P54** naringenin-7-O-glucoside, **P60** violanthin, **P67** pallidiflorin, **P69** isoliquiritigenin [31–33], **P63** licorice glycoside B/D1, **P64** licorice glycoside C2, **P66** licorice glycoside E, **P75** naringenin [34], **P53** choerospodin [35], **P62** ononin/ononin isomer [36], **P90** glyasperin C [37],and **P93** sophoraisoflavone A/semilicoisoflavone B [38]). Different from sophorae, the flavonoids in glycyrrhiza were more abundant, including chalcone, flavones, and flavanones. However, the primary cracking patterns such as neutral loss of glycosides were similar. In addition to flavonoids, triterpenoid saponins were characteristic components as well. Representative compound licorice saponin A3 (P73, $[M - H]^-$ at *m/z* of 983.4455, $[M + H]^+$ at *m/z* of 985.4644) observed fragments ions at $[M\text{-GlcA} + H]^+$ at *m/z* of 809, $[M\text{-Glc-GlcA} + H]^+$ at *m/z* of 647, $[M\text{-2GlcA-}H_2O + H]^+$ at *m/z* of 615, [M-Glc-

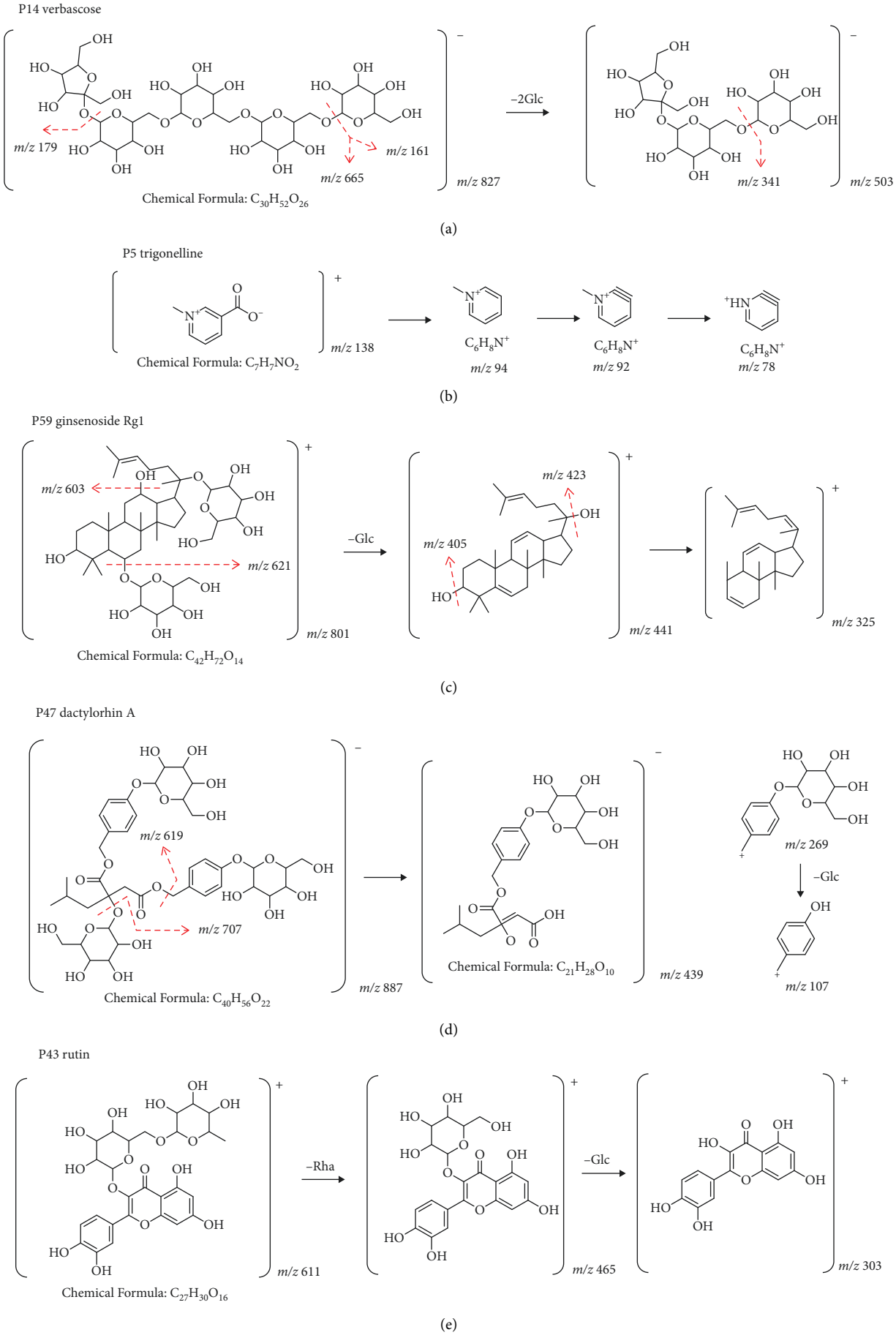

Figure 4: Continued.

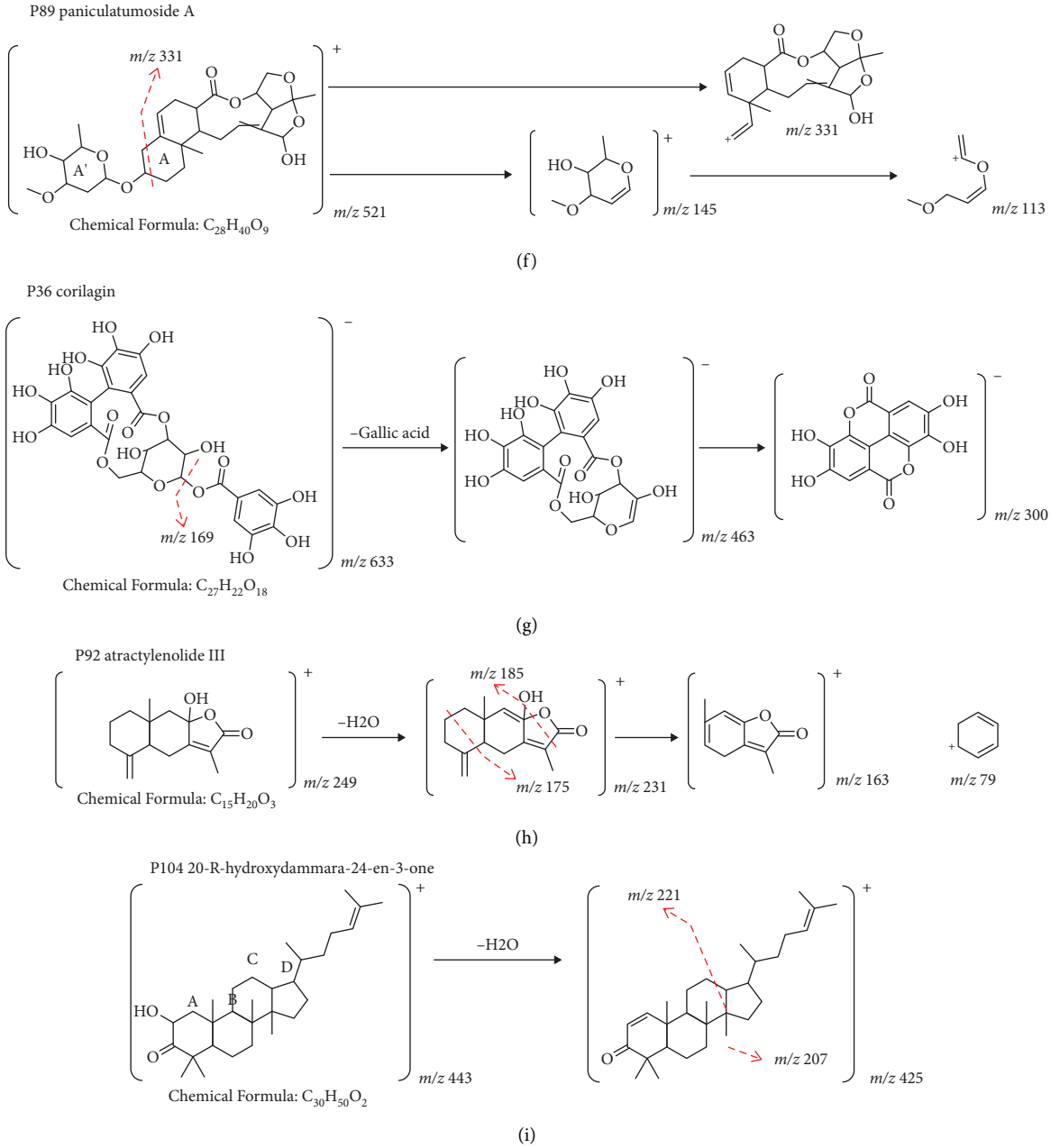

Figure 4: MS/MS spectrum and major fragmentation pathways of representative structure in LCD. (a) P14 verbascose; (b) P5 trigonelline; (c) P59 ginsenoside Rg1; (d) P47 dactylorhin A; (e) P43 rutin; (f) P89 paniculatumoside A; (g) P36 corilagin; (h) P92 atractylenolide III; (i) P104 20-R-hydroxydammara-24-en-3-one.

2GlcA + H]$^+$ at *m/z* of 471, and [M-Glc-2GlcA-H_2O + H]$^+$ at *m/z* of 453. The fragmentation pathways were similar to P59 drawn in Figure 4(c).

3.2.6. Cynanchi Paniculati Radix et Rhizoma-Derived Compounds. Only one special saponin (steroidal glycoside), namely paniculatumoside A or B (**P89**) [39], was identified in Cynanchi Paniculati Radix et Rhizoma. The cracking mainly occurred at A (*m/z* of 331) and A' rings (*m/z* of 145, 113). The typical fragmentation pathways of **P89** are drawn in Figure 4(f).

3.2.7. Typhae Pollen-Derived Compounds. In this experiment, the characteristic components detected in Typhae Pollen were flavonoids (**P42** typhaneoside [40], **P43** rutin [23–25], **P49** isorhamnetin-3-O-rutinoside-7-O-rhamnoside [24], **P50** narcissin [24, 28], and **P52** isorhamnetin-3-O-beta-galactoside [40]) and carboxylic acids (**P9** L-malic acid [23, 40], **P10** citric acid [40], **P18** succinic acid [40], **P27** 3,4-dihydroxybenzoic acid, **P51** vanillic acid [23], and **P68** decanedioic acid [41]).

Typhaneoside (P42), [M-H]$^-$ at *m/z* of 769.2194, [M +H]$^+$ at *m/z* of 771.2327) was a flavonol, and fragment ions were observed after successive loss of Rha (146 Da) and

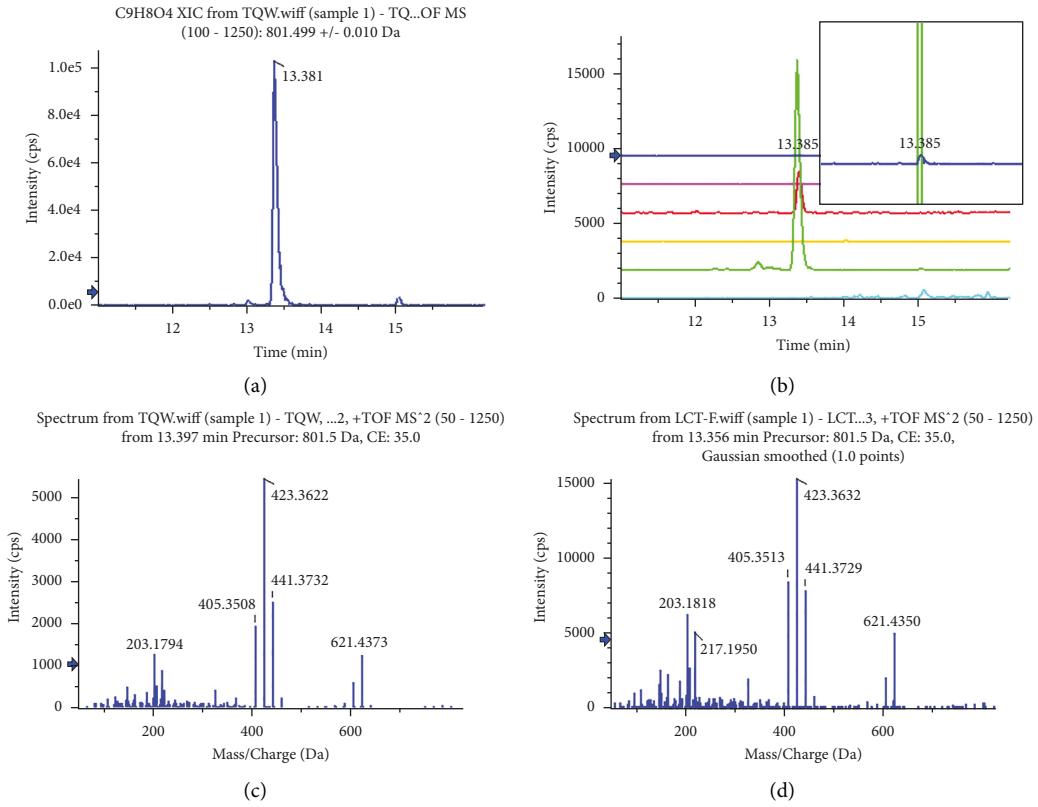

Figure 5: Identification of prototypes in bio-samples, and P59 ginsenoside Rg1 is taken as an example. (a) XIC of ginsenoside Rg1 in LCD; (b) multiple XICs of ginsenoside Rg1 in bio-samples. From top to bottom: administration plasma, blank plasma, administration urine, blank urine, administration feces, and blank feces. Ginsenoside Rg1 showed the highest intensity in feces, lowest in plasma, and no response in blank samples; (c) MS/MS spectrum of ginsenoside Rg1 in LCD; (d) MS/MS spectrum of ginsenoside Rg1 in feces.

Glc (162 Da). The fragmentation pathways were similar to P43 drawn in Figure 4(e). Simple carboxylic acids were generally responded in the negative mode, and neutral loss of·CH3 (15 Da), H2O (-18 Da), and CO_2 (-44 Da) was the most usual fragments.

3.2.8. Chebulae Fructus-Derived Compounds. In Chebulae Fructus, gallic acid structure was found in carboxylic acids (**P13** chebulic acid [42], **P23** gallic acid [23, 43], **P26** 5-galloylshikimic acid [44], **P33** brevifolincarboxylic acid [45], and **P40** 3,4,8,9,10-pentahydroxydibenzo[b,d]pyran-6-one [44]), while ellagic acid (gallic acid dimer) structure was tannins (**P28** hamamelitannin [46], **P29** 1,6-di-O-galloyl-*β*-D-glucose [47], **P34** chebulanin(1-O-galloyl-2,4-O-chebuloyl-b-D-Glc [44]), **P36** corilagin [48], and **P41** chebulagic acid [46]). Thus, ellagic acid fragment (*m/z* of 300) and neutral loss of gallic acid (170 Da) could be generally observed. The typical fragmentation pathways of **P36** corilagin are drawn in Figure 4(g).

3.2.9. Atractylodis Macrocephalae Rhizoma-Derived Compounds. The characteristic compound in Atractylodis Macrocephalae Rhizoma was lactone (**P92** atractylenolide III [11, 49]). Lactone was generally responded in the positive mode. Atractylenolide III (P92, $[M + H]^+$ at *m/z* of 249.1487) showed fragment ions at $[M\text{-}H_2O + H]^+$ at *m/z* of 231, $[M\text{-}H_2CO_2\text{+}H]^+$ at *m/z* of 185, $[M\text{-}C_3H_4O + H]^+$ at *m/z* of 175, $C_{10}H_{10}O_2{}^+$ at *m/z* of 163, and $C_6H_7{}^+$ at *m/z* of 79. The typical fragmentation pathways of **P92** atractylenolide III are drawn in Figure 4(h).

3.2.10. Coicis Semen-Derived Compounds. A total of 15 compounds could be attributed to coicis semen, including 10 carboxylic acid (**P9** L-malic acid [23, 40], **P23** gallic acid [23, 43], **P51** vanillic acid [23], **P95** pseudolaroside B, **P96** quinic acid [23], **P97** protocatechuic acid [50], **P98** caffeic acid [50], **P99** nonanedioic acid [51], **P100** 1-caffeoylquinic acid [52], and **P101** 3-O-feruloylquinic acid [52]), 3 flavonoids (**P43** rutin [23–25], **P70** quercetin [23, 29, 30],and **P103** kaempferol [29, 50]), 1 phenylpropanoid (**P19** p-coumaric acid [11, 53]), and 1 nucleoside (**P102** adenosine [53]).

3.2.11. Ailanthi Cortex-Derived Compounds. In Ailanthi Cortex, 4 compounds were attributed: briefly, 2 flavonoids (**P70** quercetin [23, 29, 30] and **P103** kaempferol [29, 50]), 1 carboxylic acid (**P99** nonanedioic acid [51]), and 1 terpene (**P104** 20-R-hydroxydammara-24-en-3-one). However, only P104 was characteristic, and it had the $[M + H]^+$ ion at *m/z* of 443.3881 and gave fragment ions at *m/z* of 425 by neutral loss of H_2O (18 Da). The crack of C ring formed ions at *m/z* of 221

Table 2: Identification of the major components present in LCD by UPLC-QTOF-MS.

No.	Compound	Formula	Rt (min)	Ion mode	Cal *m/z*	ESI-*m/z*	ppm	Fragment ions (*m/z*)	Ion mode	Cal *m/z*	ESI+*m/z*	ppm	Fragment ions (*m/z*)	Compound class	Source	Reference
P1	Choline	$C_5H_{13}NO$	1.25	—	—	—	—	—	$[M+H]^+$	104.1070	104.1065	−4.8	60, 59	Choline	CR	[11]
P2	Arginine	$C_6H_{14}N_4O_2$	1.21	$[M-H]^-$	173.1039	173.1040	0.6	173.131	$[M+H]^+$	175.1190	175.1189	−0.6	130, 116, 70, 60	Amino acid	CR	[11]
P3	Asparagine	$C_4H_8N_2O_3$	1.24	$[M-H]^-$	131.0457	131.0462	3.8	114, 113, 95, 72.58	$[M+H]^+$	133.0608	133.0606	−1.5	74	Amino acid	CR	[11]
P4	Fructose	$C_6H_{12}O_6$	1.33	$[M-H]^-$	179.0556	179.0555	−0.6	161, 131, 101, 85, 59	$[M+Na]^+$	203.0526	203.0524	−1.0	158.88.70	Saccharides	CR	[11]
P5	Trigonelline*	$C_7H_7NO_2$	1.36	—	—	—	—	—	$[M+H]^+$	138.0550	138.0546	−2.9	94, 92, 78,	Alkaloids	CR	[11]
P6	Sucrose	$C_{12}H_{22}O_{11}$	1.43	$[M-H]^-$	341.1089	341.1089	0.0	179, 89	—	—	—	—	—	Saccharides	CR	[11]
P7	Raffinose	$C_{18}H_{32}O_{16}$	1.51	$[M-H]^-$	503.1618	503.1606	−2.4	323, 191, 179	[M + NH4]+	522.2029	522.2019	−1.9	325, 289, 163, 145, 127	Saccharides	CR	[11]
P8	Stachyose	$C_{24}H_{42}O_{21}$	1.65	$[M-H]^-$	665.2146	665.2133	−2.0	341, 323, 179, 161	[M + NH4]+	684.2557	684.2549	−1.2	487, 325, 289, 163, 145, 127	Saccharides	CR	[11]
P9	L-Malic acid	$C_4H_6O_5$	1.66	$[M-H]^-$	133.0142	133.0142	0.0	115, 89, 71	—	—	—	—	—	Carboxylic acids	TP/CS	[23, 40]
P10	Citric acid	$C_6H_8O_7$	1.69	$[M-H]^-$	191.0197	191.0200	1.6	111, 85, 73	—	—	—	—	—	Carboxylic acids	TP	[40]
P11	Valine	$C_5H_{11}NO_2$	1.69	—	—	—	—	—	$[M+H]^+$	118.0863	118.0854	−7.6	72, 55	Amino acid	TP	[41]
P12	Adenine nucleoside	$C_{10}H_{13}N_5O_4$	1.76/3.20	—	—	—	—	—	$[M+H]^+$	268.1040	268.1038	−0.7	136, 119	Nucleoside	CR	[11]
P13	Chebulic acid*	$C_{14}H_{12}O_{11}$	1.80/2.27	$[M-H]^-$	355.0307	355.0296	−3.1	337, 293, 249, 205	—	—	—	—	—	Carboxylic acids	CF	[42]
P14	Verbascose	$C_{30}H_{52}O_{26}$	2.00	$[M-H]^-$	827.2669	827.2674	0.6	665, 503, 341, 179, 161	$[M+Na]^+$	851.2639	851.2618	−2.5	689	Saccharides	CR	[11]
P15	Isoleucine	$C_6H_{13}NO_2$	2.07	—	—	—	—	—	[M + H]+	132.1019	132.1013	−4.5	86, 85	Amino acid	CR	[11]
P16	L-Pyroglutamic acid	$C_5H_7NO_3$	2.41	$[M-H]^-$	128.0348	128.0353	3.9	82	[M + H]+	130.0499	130.0493	−4.6	84.56	Amino acid	CR	[11]
P17	Uridine	$C_9H_{12}N_2O_6$	2.66	$[M-H]^-$	243.0623	243.0623	0.0	200, 152, 110	[M + H]+	245.0768	245.0770	0.8	113, 70	Nucleoside	TP	[12]
P18	Succinic acid	$C_4H_6O_4$	2.70	$[M-H]^-$	117.0193	117.0192	−0.9	73	—	—	—	—	—	Carboxylic acids	TP	[40]
P19	p-Coumaric acid	$C_9H_8O_3$	2.86	—	—	—	—	—	[M + H]+	165.0546	165.0541	−3.0	162.123.77	Phenylpropanoids	CR/CS	[11, 53]
P20	Leucine	$C_6H_{13}NO_2$	3.10	—	—	—	—	—	[M + H]+	132.1019	132.1014	−3.8	86	Amino acid	TP	[41]
P21	Guanosine	$C_{10}H_{13}N_5O_5$	3.74	$[M-H]^-$	282.0838	282.0841	1.1	150, 133, 107	—	—	—	—	—	Nucleoside	CR/TP	[11, 12]
P22	Gastrodin	$C_{13}H_{18}O_7$	3.85	—	—	—	—	—	[M + NH4]+	304.1391	304.1396	1.6	108, 107, 105	Glycoside	BR	[17]
P23	Gallic acid*	$C_7H_6O_5$	4.17	$[M-H]^-$	169.0142	169.0146	2.4	125	$[M+H]^+$	171.0288	171.0281	−4.1	153, 107	Carboxylic acids	CF/CS	[23, 43]
P24	Phenylalanine	$C_9H_{11}NO_2$	5.12	$[M-H]^-$	164.0717	164.0718	0.6	147, 103, 72	$[M+H]^+$	166.0863	166.0859	−2.4	120, 103, 77	Amino acid	TP	[41]
P25	Codonopsine	$C_{14}H_{21}NO_4$	6.27	—	—	—	—	—	$[M+H]^+$	268.1543	268.1546	1.1	161, 121, 88, 58	Alkaloids	CR	[11]
P26	5-Galloylshikimic acid	$C_{14}H_{14}O_9$	6.74	$[M-H]^-$	325.0565	325.0570	1.5	169, 125	—	—	—	—	—	Carboxylic acids	CF	[44]
P27	3, 4-Dihydroxybenzoic acid	$C_7H_6O_4$	6.93	$[M-H]^-$	153.0193	153.0197	2.6	109, 108	—	—	—	—	—	Carboxylic acids	TP	—
P28	Hamamelitannin	$C_{20}H_{20}O_{14}$	7.95	$[M-H]^-$	483.0780	483.0773	−1.4	271, 211, 169, 125	—	—	—	—	—	Tannins	CF	[46]
P29	1, 6-Di-O-galloyl-β-D-glucose	$C_{20}H_{20}O_{14}$	8.52/ 8.91/ 9.09/9.25	$[M-H]^-$	483.0780	483.0779	−0.2	423, 271, 211, 169	—	—	—	—	—	Tannins	CF	[47]
P30	5-Hydroxyferulic acid	$C_{10}H_{10}O_5$	8.99	$[M-H]^-$	209.0456	209.0461	2.4	165, 121, 59	—	—	—	—	—	Carboxylic acids	AMR	-
P31	4-Hydroxybenzoic acid	$C_7H_6O_3$	9.16	$[M-H]^-$	137.0244	137.0241	−2.2	93	—	—	—	—	—	Carboxylic acids	BR	[16]
P32	Soyamaloside C	$C_{23}H_{32}O_{16}$	9.61	$[M-H]^-$	563.1618	563.1614	−0.7	461, 419	—	—	—	—	—	Glycoside	SF	[19]
P33	Brevifolincarboxylic acid	$C_{13}H_8O_8$	9.73	$[M-H]^-$	291.0141	291.0147	2.1	247, 219, 191	—	—	—	—	—	Carboxylic acids	CF	[45]
P34	Chebulanin(1-O-galloyl-2, 4-O-chebuloyl-b-D-Glc)	$C_{27}H_{24}O_{19}$	9.98	$[M-H]^-$	651.0834	651.0839	0.8	633, 481, 275, 169	—	—	—	—	—	Tannins	CF	[44]
P35	6, 7-Dihydroxycoumarin*	$C_9H_6O_4$	10.04	$[M-H]^-$	177.0188	177.0192	2.3	177, 133, 105, 89	—	—	—	—	—	Coumarins	GRR	[34]
P36	Corilagin*	$C_{27}H_{22}O_{18}$	10.18	$[M-H]^-$	633.0704	633.0732	4.4	463, 300, 169	[M + NH4]+	652.1145	652.1140	−0.7	465, 363, 303, 277	Tannins	CF	[48]
P37	Quercetin 3-O-glucosyl-rutinoside	$C_{33}H_{40}O_{21}$	10.37	$[M-H]^-$	771.1993	771.1990	−0.4	300	$[M+H]^+$	773.2136	773.2134	−0.3	465, 303	Flavonoids	SF	[21]
P38	Euphormisin M3	$C_{27}H_{24}O_{18}$	10.55	$[M-H]^-$	635.0890	635.0891	0.2	483, 465, 169, 125	[M + NH4]+	654.1301	654.1280	−3.3	467, 297, 171, 153	Glycoside	CF	[46]
P39	Manghaslin	$C_{33}H_{40}O_{20}$	10.58	$[M-H]^-$	755.2040	755.2041	0.1	609, 447, 299	$[M+H]^+$	757.2187	757.2179	−1.0	661, 449, 303	Flavonoids	SF	[22]
P40	3,4,8,9,10-Pentahydroxydibenzo [b,d]pyran-6-one	$C_{13}H_8O_7$	10.96	$[M-H]^-$	275.0192	275.0201	3.3	258, 257, 229, 201, 173, 145,	—	—	—	—	—	Carboxylic acids	CF	[44]
P41	Chebulagic acid	$C_{41}H_{30}O_{27}$	11.05	$[M-H]^-$	953.0896	953.0903	0.7	301, 275	—	—	—	—	—	Tannins	CF	[46]
P42	Typhaneoside*	$C_{34}H_{42}O_{20}$	11.25	$[M-H]^-$	769.2197	769.2194	−0.4	623, 314, 189	$[M+H]^+$	771.2343	771.2327	−2.1	625, 479, 317	Flavonoids	TP	[40]

Table 2: Continued.

No.	Compound	Formula	Rt (min)	Ion mode	Cal *m/z*	ESI-*m/z*	ppm	Fragment ions (*m/z*)	Ion mode	Cal *m/z*	ESI+*m/z*	ppm	Fragment ions (*m/z*)	Compound class	Source	Reference
P43	Rutin*	$C_{27}H_{30}O_{16}$	11.56	$[M-H]^-$	609.1461	609.1459	−0.3	301	$[M+H]^+$	611.1607	611.1607	−0.1	465, 303, 85, 71	Flavonoids	SF/TP/CS	[23–25]
P44	Licuraside/liquiritin apioside	$C_{26}H_{30}O_{13}$	11.65	$[M-H]^-$	549.1608	549.1611	0.5	255,135	$[M+H]^+$	551.1765	551.1741	−4.4	257,137	Flavonoids	GRR	[31]
P45	Hyperoside*	$C_{21}H_{20}O_{12}$	11.87	$[M-H]^-$	463.0882	463.0869	−2.8	300, 301	$[M+H]^+$	465.1028	465.1021	−1.5	303	Flavonoids	SF	[26]
P46	Liquiritin*	$C_{21}H_{22}O_9$	11.85	$[M-H]^-$	417.1191	417.1184	−1.7	255, 135	$[M+NH4]^+$	436.1603	436.1592	−2.5	257, 137	Flavonoids	GRR	[31]
P47	Dactylorhin A	$C_{40}H_{56}O_{22}$	12.06	$[M-H]^-$	887.3190	887.3181	−1.0	707, 619, 439	$[M+NH4]^+$	906.3603	906.3601	−0.3	621, 537, 459, 431, 403, 375, 325, 297, 269, 213, 191, 107	Lignans	BR	[16]
P48	Nicotiflorin*	$C_{27}H_{30}O_{15}$	12.18	$[M-H]^-$	593.1512	593.1502	−1.7	285	$[M+H]^+$	595.1658	595.1657	−0.2	449, 431, 287	Flavonoids	SF	[27]
P49	Isorhamnetin-3-O-rutinoside-7-O-rhamnoside	$C_{34}H_{40}O_{20}$	12.23	$[M-H]^-$	767.2040	767.2046	0.8	705, 665, 623, 314, 299, 271, 179	—	—	—	—	—	Flavonoids	TP	[24]
P50	Narcissin	$C_{28}H_{32}O_{16}$	12.27	$[M-H]^-$	623.1618	623.1600	−2.9	315, 314, 300, 285, 271, 255, 151	$[M+H]^+$	625.1763	625.1754	−1.4	317	Flavonoids	TP/SF	[24, 28]
P51	Vanillic acid	$C_8H_8O_4$	12.60	$[M-H]^-$	167.0350	167.0347	−1.8	152,108	—	—	—	—	—	Carboxylic acids	TP/CS	[23]
P52	Isorhamnetin-3-O-beta-galactoside	$C_{22}H_{22}O_{12}$	12.70	$[M-H]^-$	477.1038	477.1027	−2.3	314, 285	$[M+H]^+$	479.1184	479.1168	−3.3	317	Flavonoids	TP	[40]
P53	Choerospodin	$C_{21}H_{22}O_{10}$	12.83	$[M-H]^-$	433.1140	433.1151	2.5	271, 151	$[M+H]^+$	435.1286	435.1268	−4.1	273, 153	Flavonoids	GRR	[35]
P54	Naringenin-7-O-glucoside	$C_{21}H_{22}O_{10}$	12.95	$[M-H]^-$	433.1140	433.1151	2.5	433, 271, 151	$[M+H]^+$	435.1286	435.1274	−2.8	153,147	Flavonoids	GRR	[31]
P55	Notoginsenoside E	$C_{48}H_{82}O_{20}$	12.96	$[M-H]^-$	977.5321	977.5308	−1.3	931	—	—	—	—	—	Saponins	NRR	[13]
P56	Gymnoside III	$C_{42}H_{58}O_{23}$	13.22	$[M-H]^-$	975.3351	975.3336	−1.5	707, 661, 439	$[M+NH4]^+$	948.3709	948.3692	−1.8	825, 663, 635, 501, 473, 395, 367, 297, 205, 107	Lignans	BR	—
P57	Lobetyolin*	$C_{20}H_{28}O_8$	13.24	—	—	—	—	—	$[M+NH4]^+$	414.2124	414.2121	−0.6	199, 155	Glycoside	CR	[11]
P58	Ginsenoside Re*	$C_{48}H_{82}O_{18}$	13.34/15.12/16.09/16.51	$[M+COOH]^-$	991.5483	991.5459	−2.4	783, 621	$[M+H]^+$	947.5577	947.5544	−3.5	767, 749, 605, 587, 443, 407, 325	Saponins	NRR	[14]
P59	Ginsenoside Rg1*	$C_{42}H_{72}O_{14}$	13.40	$[M+COOH]^-$	845.4904	845.4899	−0.6	799, 637	$[M+H]^+$	801.4998	801.4983	−1.8	621, 603, 441, 423, 405, 325	Saponins	NRR	[14]
P60	Violanthin	$C_{27}H_{30}O_{14}$	13.65	$[M-H]^-$	577.1563	577.1553	−1.7	515, 475, 433, 145	$[M+H]^+$	579.1708	579.1701	−1.2	453, 291, 147	Flavonoids	GRR	[31]
P61	Militarine	$C_{34}H_{46}O_{17}$	13.65	$[M+COOH]^-$	771.2717	771.2702	−1.9	725, 457, 285, 153	$[M+NH4]^+$	744.3075	744.3069	−0.8	107	Lignans	BR	[17]
P62	Ononin/ononin isomer	$C_{22}H_{22}O_9$	13.73	—	—	—	—	—	$[M+H]^+$	431.1342	431.1337	−1.2	269	Flavonoids	GRR	[36]
P63	Licorice glycoside B/D1	$C_{35}H_{36}O_{15}$	13.73	$[M-H]^-$	695.1981	695.1961	−2.9	255, 399, 531, 549	—	—	—	—	—	Flavonoids	GRR	[34]
P64	Licorice glycoside C2	$C_{36}H_{38}O_{16}$	13.81	$[M-H]^-$	725.2087	725.2076	−1.5	549, 531, 255, 193	$[M+H]^+$	727.2233	727.2233	0.0	309,297,245	Flavonoids	GRR	[34]
P65	N, N′-diferuloylputrescine	$C_{24}H_{28}N_2O_6$	14.17	$[M-H]^-$	439.1875	439.1885	2.3	289, 149	$[M+H]^+$	441.2020	441.2009	−2.5	265, 177	Amino acid	SF	[18]
P66	Licorice glycoside E	$C_{35}H_{35}NO_{14}$	14.34	$[M-H]^-$	692.1985	692.1983	−0.3	549, 531	$[M+H]^+$	694.2130	694.2114	−2.3	240, 144	Flavonoids	GRR	[34]
P67	Pallidiflorin	$C_{16}H_{12}O_4$	14.42	$[M-H]^-$	267.0663	267.0661	−0.7	267, 252, 195, 132	—	—	—	—	—	Flavonoids	GRR	[31]
P68	Decanedioic acid	$C_{10}H_{18}O_4$	14.45	$[M-H]^-$	201.1132	201.1125	−3.5	183, 139,	—	—	—	—	—	Carboxylic acids	TP	[41]
P69	Isoliquiritigenin	$C_{15}H_{12}O_4$	14.46	$[M-H]^-$	255.0663	255.0655	−3.1	255, 135, 119, 91	$[M+H]^+$	257.0808	257.0816	3.1	257, 147, 137, 119, 81	Flavonoids	GRR	[31]
P70	Quercetin*	$C_{15}H_{10}O_7$	14.67	$[M-H]^-$	301.0354	301.0346	−2.7	179, 151	$[M+H]^+$	303.0499	303.0503	1.3	245, 301, 106, 151	Flavonoids	SF/CS/AC	[23, 29, 30]
P71	Licorice saponin A3	$C_{48}H_{72}O_{21}$	14.69	$[M-H]^-$	983.4493	983.4455	−3.9	821, 645, 351	$[M+H]^+$	985.4642	985.4644	0.3	809, 647, 615, 471, 453	Saponins	GRR	[31]
P72	Ginsenoside Rb1*	$C_{54}H_{92}O_{23}$	15.13	$[M+HCOOH-2H]^{2-}$	599.2997	599.2987	−1.7	1107, 945, 783, 553, 161	$[M+H]^+$	1109.6106	1109.6078	−2.5	767, 649, 605, 487, 425, 407, 325, 289	Saponins	NRR	[14]
P73	Licorice saponin G2	$C_{42}H_{62}O_{17}$	15.24	$[M-H]^-$	837.3914	837.3898	−1.9	351	$[M+H]^+$	839.4062	839.4046	−1.9	839, 663, 487, 469	Saponins	GRR	[31]
P74	Notoginsenoside R2	$C_{41}H_{70}O_{13}$	15.31	$[M+COOH]^-$	815.4799	815.4787	−1.5	769, 637	—	—	—	—	—	Saponins	NRR	[13]
P75	Naringenin*	$C_{15}H_{12}O_5$	15.57	$[M-H]^-$	271.0604	271.0612	3.0	151, 119	$[M+H]^+$	273.0757	273.0760	1.1	153, 147	Flavonoids	GRR	[34]
P76	20S-Ginsenoside Rh1*	$C_{36}H_{62}O_9$	15.71	$[M+COOH]^-$	683.4376	683.4359	−2.5	673, 475	—	—	—	—	—	Saponins	NRR	[15]

Table 2: Continued.

No.	Compound	Formula	Rt (min)	Ion mode	Cal *m/z*	ESI-*m/z*	ppm	Fragment ions (*m/z*)	Ion mode	Cal *m/z*	ESI+*m/z*	ppm	Fragment ions (*m/z*)	Compound class	Source	Reference
P77	Ginsenoside Rh4/Rk3	$C_{36}H_{60}O_8$	15.76	—	—	—	—	—	$[M+H]^+$	621.4364	621.4361	−0.4	441, 423, 405, 221, 203, 187	Saponins	NRR	[15]
P78	Licorice saponin G2 isomer	$C_{42}H_{62}O_{17}$	15.83	$[M-H]^-$	837.3914	837.3901	−1.6	351	$[M+H]^+$	839.4062	839.4065	0.3	839, 663, 645, 487, 469	Saponins	GRR	[31]
P79	Isorhamnetin*	$C_{16}H_{12}O_7$	15.95	—	—	—	—	—	$[M+H]^+$	317.0656	317.0659	0.9	302, 153	Flavonoids	SF	[22]
P80	Raho glycyrrhizin	$C_{48}H_{72}O_{20}$	15.96	$[M-H]^-$	967.4544	967.4517	−2.8	329	$[M+H]^+$	969.4692	969.4650	−4.4	621, 453, 435, 405, 217	Saponins	GRR	[32]
P81	Betulin	$C_{30}H_{50}O_2$	16.10	$[M-H]^-$	—	—	—	—	$[M+H]^+$	443.3884	443.3886	0.5	443, 425, 407, 271, 207, 175, 59	Triterpenoids	SF	[20]
P82	Ginsenoside Rd*	$C_{48}H_{82}O_{18}$	16.11	$[M+COOH]^-$	991.5483	991.5459	−2.4	783, 621	—	—	—	—	—	Saponins	NRR	[13]
P83	Yunganoside G1	$C_{48}H_{74}O_{21}$	16.14	—	—	—	—	—	$[M+H]^+$	987.4798	987.4779	−1.9	841, 665, 629, 471, 453, 441, 353	Saponins	GRR	[33]
P84	Glycyrrhizic acid*	$C_{42}H_{62}O_{16}$	16.31	$[M-H]^-$	821.3965	821.3942	−2.8	759, 351, 193	$[M+H]^+$	823.4113	823.4111	−0.2	823, 647, 471, 453, 194	Saponins	GRR	[31]
P85	Glycyrrhizic isomer /uralsaponin A/licorice saponin K2/licorice saponin H2	$C_{42}H_{62}O_{16}$	16.82/ 17.02	$[M-H]^-$	821.3965	821.3953	−1.5	351, 193	$[M+H]^+$	823.4113	823.4111	−0.2	823, 647, 471, 453, 194	Saponins	GRR	[31]
P86	Kaikasaponin III	$C_{48}H_{78}O_{17}$	17.15	$[M+COOH]^-$	971.5221	971.5194	−2.8	925	$[M+NH4]^+$	944.5580	944.5553	−2.9	503, 485, 425, 407, 309, 287, 147	Saponins	SF	[19]
P87	Uralsaponin C/licorice saponin J2	$C_{42}H_{64}O_{16}$	17.22	—	—	—	—	—	$[M+H]^+$	825.4270	825.4248	−2.6	825, 613, 455, 409, 397, 317, 177, 159, 141	Saponins	GRR	[31]
P88	Kaikasaponin I	$C_{42}H_{68}O_{13}$	17.73	—	—	—	—	—	$[M+NH4]^+$	798.5001	798.4988	−1.6	425, 407, 339, 163	Saponins	SF	[19]
P89	Paniculatumoside A/ paniculatumoside B	$C_{28}H_{40}O_9$	18.00	—	—	—	—	—	[M+H]+	521.2747	521.2739	−1.5	331, 145, 113	Saponins (steroidal glycoside)	CPRR	[39]
P90	Glyasperin C	$C_{21}H_{24}O_5$	18.09	—	—	—	—	—	$[M+H]^+$	357.1697	357.1693	−1.1	283, 165, 137, 123	Flavonoids	GRR	[37]
P91	Ginsenoside F2	$C_{42}H_{72}O_{13}$	18.57	$[M-H]^-$	779.4587	779.4575	−1.5	799	$[M+Na]^+$	807.4868	807.4835	−4.1	785, 767, 443, 407, 325	Saponins	NRR	[15]
P92	Atractylenolide III	$C_{15}H_{20}O_3$	18.62	—	—	—	—	—	$[M+H]^+$	249.1497	249.1487	−4.0	231, 175, 163, 185, 161, 105, 79	Lactone	CR/ AMR	[11, 49]
P93	Sophoraisoflavone A/ semilicoisoflavone B	$C_{20}H_{16}O_6$	19.91	—	—	—	—	—	$[M+H]^+$	353.1020	353.1018	−0.6	335, 311, 299, 215, 199, 153	Flavonoids	GRR	[38]
P94	7-[4-(11-hydroxy-undecyloxy)-phenyl]-7-pyridin-3-yl-hept-6-enoic acid ethyl ester	$C_{31}H_{45}NO_4$	20.82	—	—	—	—	—	$[M+H]^+$	496.3421	496.3392	−5.8	478, 184, 104	Esters	AMR	[49]
P95	Pseudolaroside B	$C_{14}H_{18}O_9$	6.73	$[M-H]^-$	329.08781	329.0883	1.49	163	—	—	—	—	—	Carboxylic acids	CS	—
P96	Quinic acid	$C_7H_{12}O_6$	1.42	$[M-H]^-$	191.05611	191.0561	−0.05	191	—	—	—	—	—	Carboxylic acids	CS	[23]
P97	Protocatechuic acid	$C_7H_6O_4$	6.93	$[M-H]^-$	153.01933	153.01936	0.20	109, 91	—	—	—	—	—	Carboxylic acids	CS	[50]
P98	Caffeic acid	$C_9H_8O_4$	10.13	$[M-H]^-$	179.03498	179.0349	−0.45	135	—	—	—	—	—	Carboxylic acids	CS	[50]
P99	Nonanedioic acid	$C_9H_{16}O_4$	13.2	$[M-H]^-$	187.09758	187.0978	1.18	187, 169, 125, 97, 57	$[M+H]^+$	189.1121	189.1122	0.53	171, 125, 97, 55	Carboxylic acids	CS/AC	[51]
P100	1-Caffeoylquinic acid	$C_{17}H_{20}O_9$	9.72	$[M-H]^-$	367.10346	367.1027	−2.07	193, 173	$[M+H]^+$	369.118	369.1183	0.81	177, 145	Carboxylic acids	CS	[52]
P101	3-O-Feruloylquinic acid	$C_{17}H_{20}O_9$	10.89	$[M-H]^-$	367.10346	367.1032	−0.71	193, 191, 173	$[M+H]^+$	369.118	369.1183	0.81	177, 145	Carboxylic acids	CS	[52]
P102	Adenosine	$C_{10}H_{13}N_5O_4$	3.35	—	—	—	—	—	$[M+H]^+$	268.104	268.1042	0.75	136	Nucleoside	CS	[53]
P103	Kaempferol	$C_{15}H_{10}O_6$	15.72	—	—	—	—	—	$[M+H]^+$	287.055	287.0552	0.70	231, 213, 165, 153, 121	Flavonoids	CS/AC	[29, 50]
P104	20-R-hydroxydammara-24-en-3-one	$C_{30}H_{50}O_2$	16.08	—	—	—	—	—	$[M+H]^+$	443.3884	443.3881	−0.68	425, 221, 207, 189, 133	Terpenes	AC	—

*: compounds verified by standards

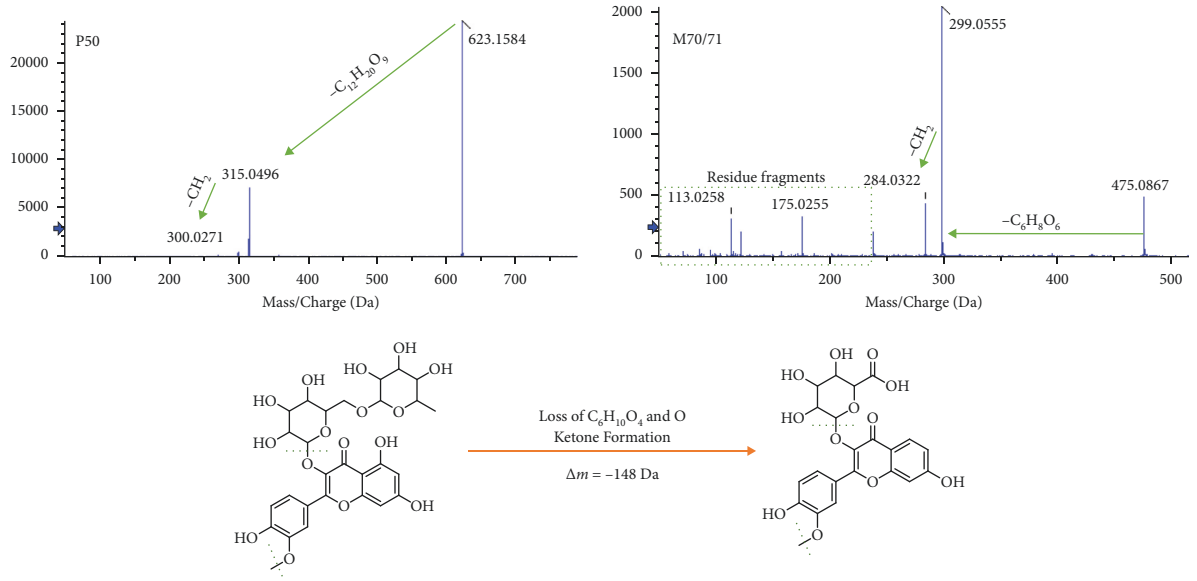

Figure 6: Identification of metabolites in bio-samples.

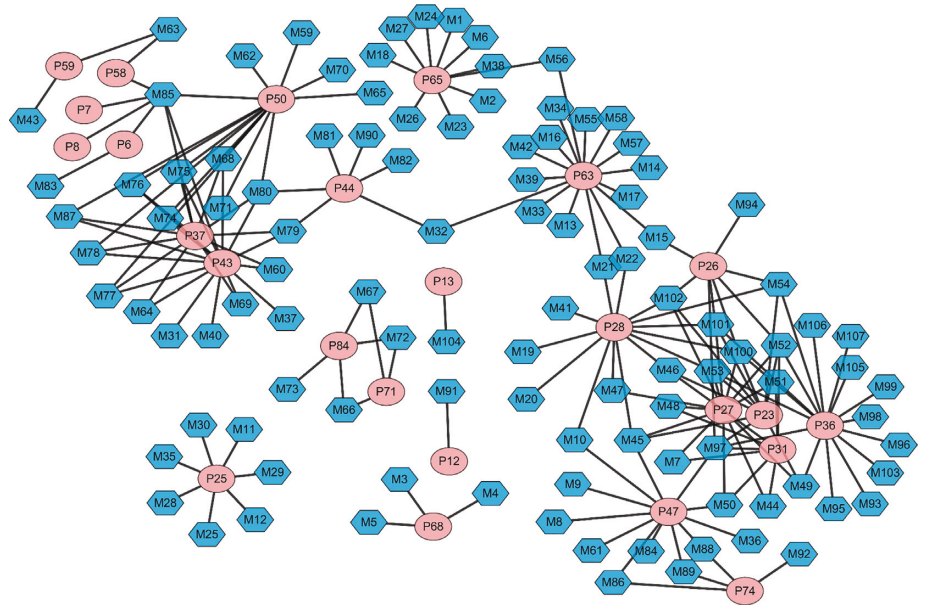

Figure 7: Correlation between prototype and metabolites.

and 207. The typical fragmentation pathways of **P104** are drawn in Figure 4(i).

3.3. Characterization of LCD-Related Xenobiotics in Rat Biological Samples. According to the compound characterization of LCD, the fragmentation patterns of mass spectrometry (accurate molecular weight and secondary debris) and retention time of chromatography were adopted to analyze the components in plasma, urine, and feces. **P59** ginsenoside Rg1 is taken as example, as shown in the XIC of LCD (Figure 5(a)) and multiple XICs of 6 bio-samples (Figure 5(b)), and a peak at 13.4 min was clearly observed in administration of bio-samples but not in the blanks. Importantly, the MS/MS spectra (*m/z* of 621, 441, 423, 405, and 203) of ginsenoside Rg1 in LCD (Figure 5(c)) and bio-samples (Figure 5(d)) were similar.

Based on the above principles, a total of 50 components were matched in biological samples, and these components would play a key role in explaining the mechanism of LCD in the future. In particular, flavonoids (**P43**, **P46**, and **P50**) and saponins (**P55** and **P72**) deserved higher attention as the five components were observed in all three bio-samples besides that were common to organisms (**P1**, **P11**, **P15**, **P24**, **P31**, and **P68**). In addition, 12 compounds were just observed in the fecal sample, mainly including some alkaloids (**P25** and **P65**), flavonoids (**P37**, **P42**, **P45**, **P52**, and **P70**), saponin (**P74**), and other small molecules (**P6**, **P9**, **P35**, and **P40**).

Table 3: Prototype and metabolic components of LCD in rat serum, urine, and fecal samples.

Metabolites	Prototype	Component name	Formula	tR (min)	Serum	Urine	Feces
—	P1	Choline	$C_5H_{13}NO$	1.25	√	√	√
—	P2	Arginine	$C_6H_{14}N_4O_2$	1.21	√	—	√
—	P3	Asparagine	$C_4H_8N_2O_3$	1.24	—	—	—
—	P4	Fructose	$C_6H_{12}O_6$	1.33	—	—	—
—	P5	Trigonelline	$C_7H_7NO_2$	1.36	√	√	—
—	P6	Sucrose	$C_{12}H_{22}O_{11}$	1.43	—	—	√
—	P7	Raffinose	$C_{18}H_{32}O_{16}$	1.51	—	—	—
—	P8	Stachyose	$C_{24}H_{42}O_{21}$	1.65	—	—	—
—	P9	L-Malic acid	$C_4H_6O_5$	1.66	—	—	√
—	P10	Citric acid	$C_6H_8O_7$	1.69	√	√	—
—	P11	Valine	$C_5H_{11}NO_2$	1.69	√	√	√
—	P12	Adenine nucleoside	$C_{10}H_{13}N_5O_4$	1.76/3.20	√	—	√
—	P13	Chebulic acid	$C_{14}H_{12}O_{11}$	1.80/2.27	—	—	—
—	P14	Verbascose	$C_{30}H_{52}O_{26}$	2.00	—	—	—
—	P15	Isoleucine	$C_6H_{13}NO_2$	2.07	√	√	√
—	P16	L-Pyroglutamic acid	$C_5H_7NO_3$	2.41	√	√	—
—	P17	Uridine	$C_9H_{12}N_2O_6$	2.66	—	—	—
—	P18	Succinic acid	$C_4H_6O_4$	2.70	√	—	√
—	P19	p-Coumaric acid	$C_9H_8O_3$	2.86	√	—	—
—	P20	Leucine	$C_6H_{13}NO_2$	3.10	√	—	—
—	P21	Guanosine	$C_{10}H_{13}N_5O_5$	3.74	—	—	—
—	P22	Gastrodin	$C_{13}H_{18}O_7$	3.85	—	√	—
—	P23	Gallic acid	$C_7H_6O_5$	4.17	—	√	√
—	P24	Phenylalanine	$C_9H_{11}NO_2$	5.12	√	√	√
—	P25	Codonopsine	$C_{14}H_{21}NO_4$	6.27	—	—	√
—	P26	5-Galloylshikimic acid	$C_{14}H_{14}O_9$	6.74	—	—	—
—	P27	3,4-Dihydroxybenzoic acid	$C_7H_6O_4$	6.93	—	√	√
—	P28	Hamamelitannin	$C_{20}H_{20}O_{14}$	7.95	—	—	—
—	P29	1,6-Di-O-galloyl-β-D-glucose	$C_{20}H_{20}O_{14}$	8.52/8.91/ 9.09/9.25	—	—	—
—	P30	5-Hydroxyferulic acid	$C_{10}H_{10}O_5$	8.99	√	√	—
—	P31	4-Hydroxybenzoic acid	$C_7H_6O_3$	9.16	√	√	√
—	P32	Soyamaloside C	$C_{23}H_{32}O_{16}$	9.61	√	—	—
—	P33	Brevifolincarboxylic acid	$C_{13}H_8O_8$	9.73	—	—	—
—	P34	Chebulanin(1-O-galloyl-2,4-O-chebuloyl-b-D-Glc)	$C_{27}H_{24}O_{19}$	9.98	—	—	—
—	P35	6,7-Dihydroxycoumarin	$C_9H_6O_4$	10.04	—	—	√
—	P36	Corilagin	$C_{27}H_{22}O_{18}$	10.18	—	—	—
—	P37	Quercetin 3-O-glucosyl-rutinoside	$C_{33}H_{40}O_{21}$	10.37	—	—	√
—	P38	Euphormisin M3	$C_{27}H_{24}O_{18}$	10.55	—	—	—
—	P39	Manghaslin	$C_{33}H_{40}O_{20}$	10.58	—	—	—
—	P40	3,4,8,9,10-Pentahydroxydibenzo[b,d]pyran-6-one	$C_{13}H_8O_7$	10.96	—	—	√
—	P41	Chebulagic acid	$C_{41}H_{30}O_{27}$	11.05	—	—	—
—	P42	Typhaneoside	$C_{34}H_{42}O_{20}$	11.25	—	—	√
—	P43	Rutin	$C_{27}H_{30}O_{16}$	11.56	√	√	√
—	P44	Licuraside/liquiritin apioside	$C_{26}H_{30}O_{13}$	11.65	—	√	√
—	P45	Hyperoside	$C_{21}H_{20}O_{12}$	11.87	—	—	√
—	P46	Liquiritin	$C_{21}H_{22}O_9$	11.85	√	√	√
—	P47	Dactylorhin A	$C_{40}H_{56}O_{22}$	12.06	√	√	—
—	P48	Nicotiflorin	$C_{27}H_{30}O_{15}$	12.18	√	—	√
—	P49	Isorhamnetin-3-O-rutinoside-7-O-rhamnoside	$C_{34}H_{40}O_{20}$	12.23	—	—	—
—	P50	Narcissin	$C_{28}H_{32}O_{16}$	12.27	√	√	√
—	P51	Vanillic acid	$C_8H_8O_4$	12.60	√	√	—
—	P52	Isorhamnetin-3-O-beta-galactoside	$C_{22}H_{22}O_{12}$	12.70	—	—	√
—	P53	Choerospodin	$C_{21}H_{22010}$	12.83	—	—	—
—	P54	Naringenin-7-O-glucoside	$C_{21}H_{22}O_{10}$	12.95	—	—	—
—	P55	Notoginsenoside E	$C_{48}H_{82}O_{20}$	12.96	√	√	√
—	P56	Gymnoside III	$C_{42}H_{58}O_{23}$	13.22	—	—	—
—	P57	Lobetyolin	$C_{20}H_{28}O_8$	13.24	—	√	—
—	P58	Ginsenoside Re	$C_{48}H_{82}O_{18}$	13.34	√	—	—
—	P59	Ginsenoside Rg1	$C_{42}H_{72}O_{14}$	13.40	√	—	√

Table 3: Continued.

Metabolites	Prototype	Component name	Formula	tR (min)	Serum	Urine	Feces
—	P60	Violanthin	$C_{27}H_{30}O_{14}$	13.65	—	√	√
—	P61	Militarine	$C_{34}H_{46}O_{17}$	13.65	√	—	—
—	P62	Ononin/Ononin isomer	$C_{22}H_{22}O_9$	13.73	—	—	—
—	P63	Licorice glycoside B/D1	$C_{35}H_{36}O_{15}$	13.73	—	—	—
—	P64	Licorice glycoside C2	$C_{36}H_{38}O_{16}$	13.81	—	—	—
—	P65	N, N′-diferuloylputrescine	$C_{24}H_{28}N_2O_6$	14.17	—	—	√
—	P66	Licorice glycoside E	$C_{35}H_{35}NO_{14}$	14.34	—	—	—
—	P67	Pallidiflorin	$C_{16}H_{12}O_4$	14.42	—	√	—
—	P68	Decanedioic acid	$C_{10}H_{18}O_4$	14.45	√	√	√
—	P69	Isoliquiritigenin	$C_{15}H_{12}O_4$	14.46	—	√	√
—	P70	Quercetin	$C_{15}H_{10}O_7$	14.67	—	—	√
—	P71	Licorice saponin A3	$C_{48}H_{72}O_{21}$	14.69	√	√	—
—	P72	Ginsenoside Rb1	$C_{54}H_{92}O_{23}$	15.13	√	√	√
—	P73	Licorice saponin G2	$C_{42}H_{62}O_{17}$	15.24	—	√	—
—	P74	Notoginsenoside R2	$C_{41}H_{70}O_{13}$	15.31	—	—	√
—	P75	Naringenin	$C_{15}H_{12}O_5$	15.57	—	—	—
—	P76	20S-Ginsenoside Rh1	$C_{36}H_{62}O_9$	15.71	—	—	—
—	P77	Ginsenoside Rh4/Rk3	$C_{36}H_{60}O_8$	15.76	—	—	—
—	P78	Licorice saponin G2 isomer	$C_{42}H_{62}O_{17}$	15.83	—	—	—
—	P79	Isorhamnetin	$C_{16}H_{12}O_7$	15.95	—	—	—
—	P80	Raho glycyrrhizin	$C_{48}H_{72}O_{20}$	15.96	—	—	—
—	P81	Betulin	$C_{30}H_{50}O_2$	16.10	—	—	—
—	P82	Ginsenoside Rd	$C_{51}H_{84}O_{21}$	16.11	—	—	—
—	P83	Yunganoside G1	$C_{48}H_{74}O_{21}$	16.14	—	—	—
—	P84	Glycyrrhizic acid	$C_{42}H_{62}O_{16}$	16.31	—	—	—
—	P85	Glycyrrhizic isomer /uralsaponin A/licorice saponin K2/ licorice saponin H2	$C_{42}H_{62}O_{16}$	16.82/17.02	—	—	—
—	P86	Kaikasaponin III	$C_{48}H_{78}O_{17}$	17.15	—	—	—
—	P87	Uralsaponin C/licorice saponin J2	$C_{42}H_{64}O_{16}$	17.22	—	—	—
—	P88	Kaikasaponin I	$C_{42}H_{68}O_{13}$	17.73	—	—	—
—	P89	Paniculatumoside A/paniculatumoside B	$C_{28}H_{40}O_9$	18.00	—	—	—
—	P90	Glyasperin C	$C_{21}H_{24}O_5$	18.09	—	—	—
—	P91	Ginsenoside F2	$C_{42}H_{72}O_{13}$	18.57	—	—	—
—	P92	Atractylenolide III	$C_{15}H_{20}O_3$	18.62	—	—	—
—	P93	Sophoraisoflavone A/semilicoisoflavone B	$C_{20}H_{16}O_6$	19.91	—	—	—
—	P94	7-[4-(11-Hydroxy-undecyloxy)-phenyl]-7-pyridin-3-yl-hept-6-enoic acid ethyl ester	$C_{31}H_{45}NO_4$	20.82	√	—	√
Total of prototypes					**29**	**27**	**34**

Metabolites	*Prototype*	*Biotransformation*	*Formula*	*tR (min)*	*Serum*	*Urine*	*Feces*
M1	P65	Loss of $C_{14}H_{17}NO_3$ + oxidation	$C_{10}H_{11}NO_4$	7.92	—	√	—
M2	P65	Loss of $C_{14}H_{17}NO_3$ + internal hydrolysis	$C_{10}H_{13}NO_4$	10.26	—	√	—
M3	P68	Desaturation	$C_{10}H_{16}O_4$	15.84	—	√	—
M4	P68	Loss of O	$C_{10}H_{18}O_3$	15.32	—	√	—
M5	P68	Loss of O + hydrogenation	$C_{10}H_{20}O_3$	16.94	√	—	—
M6	P65	Loss of $C_{14}H_{18}N_2O_3$ + ketone formation	$C_{10}H_8O_4$	12.16	—	√	—
M7	P27 P31	Loss of O + glucuronidation Glucuronidation	$C_{13}H_{14}O_9$	10.48	—	√	—
M8	P47	Loss of $C_{27}H_{38}O_{16}$ + ketone formation	$C_{13}H_{16}O_7$	11.22	√	√	—
M9	P47	Loss of $C_{27}H_{38}O_{16}$ and O	$C_{13}H_{18}O_5$	15.34	—	√	—
M10	P28 P47	Loss of O and $C_7H_4O_5$ + hydrogenation Loss of $C_{27}H_{38}O_{15}$ + oxidation	$C_{13}H_{18}O_8$	8.74	—	√	—
M11	P25	Loss of CH_2	$C_{13}H_{19}NO_4$	6.13	—	√	—
M12	P25	Loss of CH_2 + sulfate conjugation	$C_{13}H_{19}NO_7S$	9.85	—	√	—
M13	P63	Loss of $C_{26}H_{28}O_{13}$ + glutamine conjugation	$C_{14}H_{16}N_2O_4$	13.77	—	√	—
M14	P63	Loss of $C_{21}H_{20}O_9$ and O	$C_{14}H_{16}O_5$	13.34	—	√	—
M15	P63 P26	Loss of $C_{21}H_{20}O_8$ Loss of O and O + hydrogenation	$C_{14}H_{16}O_7$	12.21	—	√	—
M16	P63	Loss of $C_{21}H_{20}O_8$ + oxidation	$C_{14}H_{16}O_8$	8.21	—	√	—
M17	P63	Loss of $C_{21}H_{20}O_8$ + oxidation	$C_{14}H_{16}O_8$	9.28	—	√	—
M18	P65	Loss of $C_{10}H_9NO_3$ + demethylation to carboxylic acid	$C_{14}H_{17}NO_5$	8.16	—	√	—

Table 3: Continued.

Metabolites	Prototype	Component name	Formula	tR (min)	Serum	Urine	Feces
M19	P28	Loss of $C_7H_4O_4$+methylation	$C_{14}H_{18}O_{10}$	4.85	—	√	—
M20	—P28	Loss of $C_7H_4O_4$ + methylation	$C_{14}H_{18}O_{10}$	5.12	—	√	—
M21	—P28 P63	Loss of O and $C_7H_4O_5$ + methylation Loss of $C_{21}H_{20}O_8$ + internal hydrolysis	$C_{14}H_{18}O_8$	7.3	—	√	—
M22	P28 P63	Loss of O and $C_7H_4O_5$ + methylation Loss of $C_{21}H_{20}O_8$ + internal hydrolysis	$C_{14}H_{18}O_8$	11.29	—	√	—
M23	P65	Loss of $C_{10}H_9NO_3$	$C_{14}H_{19}NO_3$	15.44	—	√	—
M24	P65	Loss of $C_{10}H_9NO_3$	$C_{14}H_{19}NO_3$	15.73	—	√	—
M25	P25	Desaturation	$C_{14}H_{19}NO_4$	14.65	—	√	—
M26	P65	Loss of $C_{10}H_8O_3$	$C_{14}H_{20}N_2O_3$	7.03	—	√	—
M27	P65	Loss of $C_{10}H_8O_3$ + phosphorylation	$C_{14}H_{21}N_2O_6P$	5.86	—	√	—
M28	P25	Oxidation	$C_{14}H_{21}NO_5$	2.32	—	—	√
M29	P25	Sulfate conjugation	$C_{14}H_{21}NO_7S$	12.22	—	√	—
M30	P25	Phosphorylation	$C_{14}H_{22}NO_7P$	10.82	—	√	—
M31	P43	Loss of $C_{12}H_{20}O_9$	$C_{15}H_{10}O_7$	14.63	—	√	√
M32	P44 P63	Loss of $C_{11}H_{18}O_9$ Loss of $C_{20}H_{24}O_{11}$	$C_{15}H_{12}O_4$	14.47	—	√	√
M33	P63	Loss of $C_{20}H_{24}O_{11}$ + oxidation	$C_{15}H_{12}O_5$	15.52	—	√	—
M34	P63	Loss of $C_{20}H_{24}O_{12}$ + internal hydrolysis	$C_{15}H_{14}O_4$	16.12	—	√	√
M35	P25	Methylation	$C_{15}H_{23}NO_4$	14.47	—	√	—
M36	P47	Loss of $C_{13}H_{16}O_7$ and $C_{13}H_{16}O_6$ + methylation	$C_{15}H_{26}O_9$	13.24	—	√	—
M37	P43	Loss of $C_{12}H_{20}O_{10}$ and O + methylation	$C_{16}H_{12}O_5$	18.12	—	√	—
M38	P65	Loss of $C_{14}H_{18}N_2O_3$ + glucose conjugation	$C_{16}H_{20}O_8$	13.53	—	√	—
M39	P63	Loss of $C_{15}H_{10}O_4$ + internal hydrolysis	$C_{20}H_{28}O_{12}$	8.03	—	√	—
M40	P43	Loss of $C_6H_{10}O_4$ + oxidation	$C_{21}H_{20}O_{13}$	9.06	—	√	—
M41	P28	Loss of O and O + methylation	$C_{21}H_{22}O_{12}$	8.03	—	√	—
M42	P63	Loss of $C_9H_6O_2$ + glucuronidation	$C_{32}H_{38}O_{19}$	9.94	—	√	—
M43	P59	Loss of O	$C_{42}H_{72}O_{13}$	15.11	√	√	√
M44	P27 P31	Loss of O and O Loss of O	$C_7H_6O_2$	12.52	—	√	—
M45	P23 P27 P28 P47	Loss of O and O Loss of O Loss of O and $C_{13}H_{14}O_{10}$ Loss of $C_{27}H_{38}O_{15}$ and $C_6H_{10}O_6$ + demethylation to carboxylic acid	$C_7H_6O_3$	13.51	√	√	—
M46	P23 P28 P31	Loss of O Loss of $C_{13}H_{14}O_{10}$ Oxidation	$C_7H_6O_4$	9.12	—	√	—
M47	P27 P28	Oxidation Loss of $C_{13}H_{14}O_9$	$C_7H_6O_5$	4.16	—	√	√
M48	P27 P31	Loss of O + sulfate conjugation Sulfate conjugation	$C_7H_6O_6S$	6.83	√	√	—
M49	P23 P36 P27	Loss of O + sulfate conjugation Loss of $C_{20}H_{16}O_{14}$ + sulfate conjugation Sulfate conjugation	$C_7H_6O_7S$	6.76	√	√	—
M50	P27 P31 P47	Loss of O and O + hydrogenation Loss of O + hydrogenation Loss of $C_{27}H_{38}O_{15}$ and $C_6H_{10}O_5$	$C_7H_8O_2$	8.01	—	√	√
M51	P27 P31 P36	Loss of O and O + methylation Loss of O + methylation Loss of $C_{20}H_{16}O_{14}$ and O + methylation	$C_8H_8O_2$	11.44	—	√	—
M52	P26 P23 P27 P31	Loss of $C_7H_8O_5$ and O + methylation Loss of O and O + methylation Loss of O + methylation Methylation	$C_8H_8O_3$	13.29	—	√	—
M53	P23 P27 P36 P28	Loss of O + methylation Methylation Loss of $C_{20}H_{16}O_{14}$ + methylation Loss of $C_{13}H_{14}O_{10}$ + methylation	$C_8H_8O_4$	12.58	√	√	—

Table 3: Continued.

Metabolites	Prototype	Component name	Formula	tR (min)	Serum	Urine	Feces
	P23	Methylation					
M54	P36	Loss of $C_{20}H_{16}O_{13}$ + methylation	$C_8H_8O_5$	8.53	√	√	√
	P26	Loss of $C_7H_8O_4$ + methylation					
	P28	Loss of $C_{13}H_{14}O_9$ + methylation					
M55	P63	Loss of $C_{26}H_{28}O_{13}$ + internal hydrolysis	$C_9H_{10}O_3$	9	√	√	—
M56	P63	Loss of $C_{26}H_{28}O_{12}$	$C_9H_8O_3$	11.56	√	√	√
	P65	Loss of CH_2 and $C_{14}H_{18}N_2O_3$					
M57	P63	Loss of $C_{26}H_{28}O_{12}$ + oxidation	$C_9H_8O_4$	14.04	—	—	√
M58	P63	Loss of $C_{26}H_{28}O_{12}$ + oxidation	$C_9H_8O_4$	9.04	—	√	—
M59	P50	Glucuronidation	$C_{34}H_{40}O_{22}$	10.68	—	√	—
M60	P37	Ketone formation	$C_{33}H_{38}O_{22}$	9.37	—	√	—
	P43	Glucuronidation					
M61	P47	Loss of $C_{13}H_{16}O_7$ and O + phosphorylation	$C_{27}H_{41}O_{17}P$	5.05	—	√	—
M62	P50	Demethylation to carboxylic acid	$C_{28}H_{30}O_{18}$	10.57	—	√	—
M63	P59	Loss of $C_6H_{10}O_6$	$C_{36}H_{62}O_8$	21.05	—	—	√
	P58	Loss of $C_{12}H_{20}O_{10}$					
M64	P37	Loss of O and $C_6H_{10}O_6$ + hydrogenation	$C_{27}H_{32}O_{14}$	13.05	—	—	√
	P43	Loss of O and O + hydrogenation					
M65	P50	Loss of $C_6H_{10}O_5$ + demethylation to carboxylic acid	$C_{22}H_{20}O_{13}$	10.6	—	√	—
M66	P84	Loss of $C_{12}H_{16}O_{12}$ + oxidation	$C_{30}H_{46}O_5$	19.88	—	—	√
	P71	Loss of $C_{12}H_{16}O_{12}$ and $C_6H_{10}O_5$ + oxidation					
M67	P84	Loss of $C_{12}H_{16}O_{12}$ + oxidation	$C_{30}H_{46}O_5$	19.47	√	—	√
	P71	Loss of $C_{12}H_{16}O_{12}$ and $C_6H_{10}O_5$ + oxidation					
	P50	Loss of $C_6H_{10}O_4$					
M68	P37	Loss of $C_{12}H_{20}O_9$ + methylation	$C_{22}H_{22}O_{12}$	13.16	√	√	—
	P43	Loss of $C_6H_{10}O_4$ + methylation					
M69	P37	Loss of $C_{12}H_{20}O_{10}$ + demethylation to carboxylic acid	$C_{21}H_{18}O_{13}$	13.13	√	√	—
	P43	Loss of $C_6H_{10}O_5$ + demethylation to carboxylic acid					
M70	P50	Loss of $C_6H_{10}O_4$ and O + ketone formation	$C_{22}H_{20}O_{12}$	12.83	—	√	—
M71	P50	Loss of $C_6H_{10}O_4$ and O + ketone formation	$C_{22}H_{20}O_{12}$	12.51	—	√	—
M72	P84	Loss of $C_{12}H_{16}O_{12}$	$C_{30}H_{46}O_4$	22.29	√	—	—
	P71	Loss of $C_{12}H_{16}O_{12}$ and $C_6H_{10}O_5$					
M73	P84	Loss of $C_{12}H_{16}O_{13}$ + ketone formation	$C_{30}H_{44}O_4$	19.47	√	√	√
	P50	Loss of $C_6H_{10}O_5$					
M74	P37	Loss of $C_{12}H_{20}O_{10}$ + methylation	$C_{22}H_{22}O_{11}$	15.04	—	√	—
	P43	Loss of $C_6H_{10}O_5$ + methylation					
	P50	Loss of $C_6H_{10}O_5$ + demethylation and methylene to ketone					
M75	P37	Loss of $C_{12}H_{20}O_{10}$ + ketone formation	$C_{21}H_{18}O_{12}$	13.1	—	√	—
	P43	Loss of $C_6H_{10}O_5$ + ketone formation					
	P50	Loss of $C_6H_{10}O_5$ + demethylation and methylene to ketone					
M76	P37	Loss of $C_{12}H_{20}O_{10}$ + ketone formation	$C_{21}H_{18}O_{12}$	12.79	—	√	—
	P43	Loss of $C_6H_{10}O_5$ + ketone formation					
	P50	Loss of $C_6H_{10}O_4$ and CH_2O					
M77	P37	Loss of $C_{12}H_{20}O_{10}$	$C_{21}H_{20}O_{11}$	13.08	√	√	—
	P43	Loss of $C_6H_{10}O_5$					
	P50	Loss of $C_6H_{10}O_4$ and CH_2O					
M78	P37	Loss of $C_{12}H_{20}O_{10}$	$C_{21}H_{20}O_{11}$	12.95	√	√	—
	P43	Loss of $C_6H_{10}O_5$					
	P44	Loss of $C_5H_8O_4$ + oxidation					
M79	P37	Loss of O and $C_{12}H_{20}O_{10}$ + hydrogenation	$C_{21}H_{22}O_{10}$	13.79	—	√	—
	P43	Loss of $C_6H_{10}O_5$ and O + hydrogenation					
	P44	Loss of $C_5H_8O_5$ + demethylation to carboxylic acid					
M80	P50	Loss of $C_6H_{10}O_5$ and CH_2O	$C_{21}H_{20}O_{10}$	11.83	√	√	—
	P37	Loss of O and $C_{12}H_{20}O_{10}$					
	P43	Loss of $C_6H_{10}O_5$ and O					
M81	P44	Loss of $C_5H_8O_5$+ketone formation	$C_{21}H_{20}O_9$	10.5	—	√	—
M82	P44	Loss of $C_5H_8O_5$+hydrogenation	$C_{21}H_{24}O_8$	13.18	—	√	—
M83	P6	Loss of $H_{-2}O$ + methylation	$C_{13}H_{26}O_{10}$	3.74	—	√	—
M84	P47	Loss of $C_{13}H_{16}O_7$ and $C_{13}H_{16}O_6$ + demethylation and methylene to ketone	$C_{13}H_{20}O_{10}$	7.5	—	√	—

Table 3: Continued.

Metabolites	Prototype	Component name	Formula	tR (min)	Serum	Urine	Feces
	P58	Loss of $C_{36}H_{60}O_9$ + methylation					
	P50	Loss of $C_{16}H_{10}O_7$ + methylation					
	P37	Loss of $C_{21}H_{18}O_{12}$ + methylation					
M85	P7	Loss of $C_6H_{10}O_6$ and O + methylation	$C_{13}H_{24}O_9$	6.42	—	√	—
	P43	Loss of $C_{15}H_8O_7$ + methylation					
	P6	Loss of O and O + methylation					
	P8	Loss of $C_6H_{10}O_6$ and $C_6H_{10}O_6$ + methylation					
M86	P47	Loss of $C_{27}H_{38}O_{15}$ + methylation	$C_{14}H_{20}O_7$	11.44	—	√	—
	P74	Loss of $C_{21}H_{28}O_{10}$ + methylation					
	P50	Loss of $C_{12}H_{20}O_9$ and CH_2O					
M87	P37	Loss of $C_{18}H_{30}O_{15}$	$C_{15}H_{10}O_6$	13.08	—	√	—
	P43	Loss of $C_{12}H_{20}O_{10}$					
M88	P47	Loss of $C_{27}H_{38}O_{16}$	$C_{13}H_{18}O_6$	10.65	—	√	√
	P74	Loss of $C_{21}H_{28}O_{11}$					
M89	P47	Loss of $C_{27}H_{38}O_{16}$ + loss of hydroxymethylene	$C_{12}H_{16}O_5$	11.17	—	√	—
	P74	Loss of $C_{21}H_{28}O_{11}$ + loss of hydroxymethylene					
M90	P44	Loss of $C_{11}H_{18}O_{10}$	$C_{15}H_{12}O_3$	10.5	—	√	—
M91	P12	Loss of O + loss of hydroxymethylene	$C_9H_{11}N_5O_2$	1.38	—	—	√
M92	P74	Loss of $C_{13}H_{16}O_6$ and $C_{13}H_{16}O_6$	$C_8H_{14}O_5$	11.2	—	√	—
M93	P36	Loss of $C_{20}H_{16}O_{13}$ + decarboxylation	$C_6H_6O_3$	6	—	√	—
M94	P26	Loss of $C_7H_4O_5$	$C_7H_{10}O_4$	14.59	—	√	—
M95	P36	Loss of $C_{20}H_{16}O_{14}$ + taurine conjugation	$C_9H_{11}NO_6S$	2.81	√	—	—
M96	P36	Loss of $C_{14}H_6O_{10}$ + demethylation and methylene to ketone	$C_{12}H_{12}O_9$	4.71	—	√	—
	P23	Loss of O and O + glucose conjugation					
	P36	Loss of $C_{14}H_6O_{10}$					
M97	P26	Loss of $C_7H_8O_5$ and O + glucose conjugation	$C_{13}H_{16}O_8$	4.11	—	√	—
	P31	Glucose conjugation					
	P47	Loss of $C_{27}H_{38}O_{16}$ + demethylation to carboxylic acid					
M98	P36	Loss of $C_{14}H_6O_{10}$ + hydrogenation	$C_{13}H_{18}O_8$	8.74	—	√	—
M99	P36	Loss of $C_{13}H_{12}O_{10}$	$C_{14}H_{10}O_8$	13.63	—	√	—
	P23	Loss of O + glucose conjugation					
	P27	Glucose conjugation					
M100	P28	Loss of $C_7H_4O_5$	$C_{13}H_{16}O_9$	6.81	√	√	—
	P36	Loss of $C_{14}H_6O_9$					
	P26	Loss of $C_7H_8O_5$ + glucose conjugation					
	P23	Loss of O + glucose conjugation					
	P27	Glucose conjugation					
M101	P28	Loss of $C_7H_4O_5$	$C_{13}H_{16}O_9$	6.57	√	√	—
	P36	Loss of $C_{14}H_6O_9$					
	P26	Loss of $C_7H_8O_5$ + glucose conjugation					
	P23	Loss of O + glucuronidation					
M102	P26	Loss of $C_7H_8O_5$ + glucuronidation	$C_{13}H_{14}O_{10}$	5.69	—	√	—
	P27	Glucuronidation					
	P28	Loss of $C_7H_4O_5$ + ketone formation					
M103	P36	Loss of $C_{14}H_6O_9$ + methylation	$C_{14}H_{18}O_9$	3.63	—	√	—
M104	P13	Loss of $H_{-2}O$ + hydrogenation	$C_{14}H_{16}O_{10}$	7.96	—	√	—
M105	P36	Loss of $C_{13}H_{12}O_8$ + methylation	$C_{15}H_{12}O_{10}$	11.93	—	√	—
M106	P36	Loss of $C_{13}H_{12}O_8$ + methylation	$C_{15}H_{12}O_{10}$	10.7	—	√	—
M107	P36	Loss of $C_{13}H_{12}O_9$ + glutamine conjugation	$C_{19}H_{18}N_2O_{11}$	14.07	—	—	√
		Total of metabolites			**22**	**96**	**18**

These compounds may not be absorbed into the blood, but are still effective in regulating gut microbiota. The detailed information about the distribution of components in plasma, urine, and feces is summarized in Table 2.

Furtherly, the phase I and phase II metabolic regularity, as well as the similarity of secondary mass spectrum profile, was used to identify the metabolite. Those metabolites were annotated through automatic matching with prototype components by MetabolitePilot Software. Briefly, MetabolitePilot operated prototype-metabolite matching through mass defect filter (MDF), characteristic product ion filter (PIF), and neutral loss filter (NLF). As shown in Figure 6, the mass defect from P50 to M70/71 was -148 Da with the biotransformation named "loss of $C_6H_{10}O_4$ and O (hydrolysis, phase I) + ketone formation (phase I)." Furthermore, neutral loss of glycosides and methylene was both observed in the

MS/MS spectra of P50 and M70/71, which implied the similar skeleton. That was to say, these compounds were structurally related, and M70/71 could be the metabolites of P50. As a result, a total of 107 metabolites were matched with 25 prototypes in plasma, urine, or feces. The network of prototype-metabolite matching is drawn as in Figure 7. The details involving the distribution and biotransformations of metabolites are listed in Table 3. It was worth noting that although some prototypes have not been observed in biosamples, they still are effective through metabolites. For example, P28 hamamelitannin produced 14 metabolites that were all detected in urine, and 5 were found in plasma and 2 in feces. It could be metabolized in the gut, and metabolites were furtherly absorbed into the bloodstream. In total, 29 prototype components and 22 metabolites were detected in plasma. About 27 prototypes and 96 metabolites were detected in urine, and 34 prototypes and 18 metabolites were detected in feces. These substances were considered to constitute the pharmacodynamic substance basis of LCD.

P2 arginine [54–56], **P5** trigonelline [57], **P59** ginsenoside Rg1 [58], **P69** isoliquiritigenin [59], **P82** ginsenoside Rd [60, 61], and **P84** glycyrrhizic acid [62–64] would alleviate the symptom of UC based on anti-inflammation or antioxidant activities. Besides, **P15** isoleucine [65], **P17** uridine [12, 66], **P21** guanosine [67], **P23** gallic acid [68, 69], **P43** rutin [70, 71], **P51** vanillic acid [72], **P70** quercetin [73, 74], **P72** ginsenoside Rb1 [75], and **P81** betulin [76]were confirmed to treat UC through NF-κB pathway. **P8** stachyose increased beneficial microbiota and bacterial diversity to alleviate colitis mice [77]. **P45** hyperoside ameliorates ulcer colitis mice through MKRN1-mediated regulation of PPARγ signaling and Th17/Treg balance [78]. The effect of those metabolisms on UC was worth to study for new drug development.

Data Availability

The data used to support the findings of this study are included within the article.

Conflicts of Interest

None.

Authors' Contributions

Baofu Lin, Shaoju Guo, and Xinxin Hong performed the experiments and wrote the manuscript. Xiaoyan Jiang, Haiwen Li, and Jingwei Li summarized and analyzed the data. Linglong Guo and Mianli Li assisted with the assay and checked the statistics. JianPing Chen, Bin Huang, and Yifei Xu designed the study and finally revised the manuscript.

Acknowledgments

This research was supported by National Science Foundation of China (82104482); Project of Administration of Traditional Chinese Medicine of Guangdong Province of China (20213015); and Shenzhen Science and Technology Plan Project (JCYJ20180302173834208).

References

[1] F. Cheung, "TCM: made in China," *Nature*, vol. 480, no. 7378, pp. S82–S83, 2011.

[2] Z. Liu, F. Guo, Y. Wang et al., "BATMAN-TCM: a bioinformatics analysis tool for molecular mechANism of traditional Chinese medicine," *Scientific Reports*, vol. 6, no. 1, Article ID 21146, 2016.

[3] Y. Han, H. Sun, A. Zhang, G. Yan, and X.-J. Wang, "Chinmedomics, a new strategy for evaluating the therapeutic efficacy of herbal medicines," *Pharmacology & Therapeutics*, vol. 216, Article ID 107680, 2020.

[4] G.-Z. Xin, L.-W. Qi, Z.-Q. Shi et al., "Strategies for integral metabolism profile of multiple compounds in herbal medicines: pharmacokinetics, metabolites characterization and metabolic interactions," *Current Drug Metabolism*, vol. 12, no. 9, pp. 809–817, 2011.

[5] J. D. Feuerstein, A. C. Moss, and F. A. Farraye, "Ulcerative colitis," *Mayo Clinic Proceedings*, vol. 94, no. 7, pp. 1357–1373, 2019.

[6] Y. Jing, A. Li, Z. Liu et al., "Absorption of Codonopsis pilosula saponins by coexisting polysaccharides alleviates gut microbial dysbiosis with dextran sulfate sodium-induced colitis in model mice," *BioMed Research International*, vol. 2018, Article ID 1781036, 2018.

[7] W. Feng, J. Liu, Y. Tan, H. Ao, J. Wang, and C. Peng, "Polysaccharides from Atractylodes macrocephala Koidz. Ameliorate ulcerative colitis via extensive modification of gut microbiota and host metabolism," *Food research international (Ottawa, Ont.)*, vol. 138, no. Pt B, Article ID 109777, 2020.

[8] S. Habtemariam and A. Belai, "Natural therapies of the inflammatory bowel disease: the case of rutin and its aglycone, quercetin," *Mini Reviews in Medicinal Chemistry*, vol. 18, no. 3, pp. 234–243, 2018.

[9] Y. Chen, R. Yu, L. Jiang et al., "A comprehensive and rapid quality evaluation method of traditional Chinese medicine decoction by integrating UPLC-QTOF-MS and UFLC-QQQ-MS and its application," *Molecules*, vol. 24, no. 2, 2019.

[10] F. Wang, S. Huang, Q. Chen et al., "Chemical characterisation and quantification of the major constituents in the Chinese herbal formula Jian-Pi-Yi-Shen pill by UPLC-Q-TOF-MS/MS and HPLC-QQQ-MS/MS," *Phytochemical Analysis*, vol. 31, no. 6, pp. 915–929, 2020.

[11] M.-H. Liu, X. Tong, J.-X. Wang, W. Zou, H. Cao, and W.-W. Su, "Rapid separation and identification of multiple constituents in traditional Chinese medicine formula Shenqi Fuzheng Injection by ultra-fast liquid chromatography combined with quadrupole-time-of-flight mass spectrometry," *Journal of Pharmaceutical and Biomedical Analysis*, vol. 74, pp. 141–155, 2013.

[12] W.-W. Tao, J.-A. Duan, N.-Y. Yang et al., "Determination of nucleosides and nucleobases in the pollen of Typha angustifolia by UPLC-PDA-MS," *Phytochemical Analysis*, vol. 23, no. 4, pp. 373–378, 2012.

[13] J. Li, R.-F. Wang, Y. Zhou et al., "Dammarane-type triterpene oligoglycosides from the leaves and stems of Panax notoginseng and their antiinflammatory activities," *Journal of Ginseng Research*, vol. 43, no. 3, pp. 377–384, 2019.

[14] Q. Xie, H. Yuan, Y. Liu et al., "Simultaneous determination of 19 bioactive constituents in QishenYiqi dropping pills by ultra-performance liquid chromatography coupled with triple quadrupole mass spectrometry," *Journal of AOAC International*, vol. 102, no. 4, pp. 1102–1111, 2019.

[15] C.-Z. Gu, J.-J. Lv, X.-X. Zhang et al., "Triterpenoids with promoting effects on the differentiation of PC12 cells from the steamed roots of Panax notoginseng," *Journal of Natural Products*, vol. 78, no. 8, pp. 1829–1840, 2015.

[16] D. Xu, Y. Pan, and J. Chen, "Chemical constituents, pharmacologic properties, and clinical applications of Bletilla striata," *Frontiers in Pharmacology*, vol. 10, p. 1168, 2019.

[17] Y. Zhao, J.-J. Niu, X.-C. Cheng et al., "Chemical constituents from Bletilla striata and their NO production suppression in RAW 264.7 macrophage cells," *Journal of Asian Natural Products Research*, vol. 20, no. 4, pp. 385–390, 2018.

[18] Y.-H. Lo, R.-D. Lin, Y.-P. Lin, Y.-L. Liu, and M.-H. Lee, "Active constituents from Sophora japonica exhibiting cellular tyrosinase inhibition in human epidermal melanocytes," *Journal of Ethnopharmacology*, vol. 124, no. 3, pp. 625–629, 2009.

[19] Y. Zhang, L. Qu, L. Liu et al., "New maltol glycosides from flos sophorae," *Journal of Natural Medicines*, vol. 69, no. 2, pp. 249–254, 2015.

[20] W. Zhang, H. Jiang, J. Yang et al., "Safety assessment and antioxidant evaluation of betulin by LC-MS combined with free radical assays," *Analytical Biochemistry*, vol. 587, Article ID 113460, 2019.

[21] R. Liu, Z. Cai, and B. Xu, "Characterization and quantification of flavonoids and saponins in adzuki bean (Vigna angularis L.) by HPLC-DAD-ESI-MSn analysis," *Chemistry Central Journal*, vol. 11, no. 1, p. 93, 2017.

[22] G. C. Kite, C. A. Stoneham, and N. C. Veitch, "Flavonol tetraglycosides and other constituents from leaves of Styphnolobium japonicum (Leguminosae) and related taxa," *Phytochemistry*, vol. 68, no. 10, pp. 1407–1416, 2007.

[23] L. Wang, C. Chen, A. Su, Y. Zhang, J. Yuan, and X. Ju, "Structural characterization of phenolic compounds and antioxidant activity of the phenolic-rich fraction from defatted adlay (Coix lachryma-jobi L . var. ma-yuen Stapf) seed meal," *Food Chemistry*, vol. 196, pp. 509–517, 2016.

[24] Y. Chen, H. Yu, H. Wu et al., "Characterization and quantification by LC-MS/MS of the chemical components of the heating products of the flavonoids extract in pollen Typhae for transformation rule exploration," *Molecules*, vol. 20, no. 10, pp. 18352–18366, 2015.

[25] M. Xu, Z. Jin, J.-B. Ohm, P. Schwarz, J. Rao, and B. Chen, "Effect of germination time on antioxidative activity and composition of yellow pea soluble free and polar soluble bound phenolic compounds," *Food & Function*, vol. 10, no. 10, pp. 6840–6850, 2019.

[26] X. Jin, Y. Lu, S. Chen, and D. Chen, "UPLC-MS identification and anticomplement activity of the metabolites of Sophora tonkinensis flavonoids treated with human intestinal bacteria," *Journal of Pharmaceutical and Biomedical Analysis*, vol. 184, Article ID 113176, 2020.

[27] H. Cedeño, S. Espinosa, J. M. Andrade, L. Cartuche, and O. Malagón, "Novel flavonoid glycosides of quercetin from leaves and flowers of gaiadendron punctatum G.don. (violeta de Campo), used by the saraguro community in southern Ecuador, inhibit α-glucosidase enzyme," *Molecules*, vol. 24, no. 23, 2019.

[28] W.-Y. Yang, T. H. Won, C.-H. Ahn et al., "Streptococcus mutans sortase A inhibitory metabolites from the flowers of Sophora japonica," *Bioorganic & Medicinal Chemistry Letters*, vol. 25, no. 7, pp. 1394–1397, 2015.

[29] J. Ryu, J. S. Kim, and S. S. Kang, "Cerebrosides from longan arillus," *Archives of Pharmacal Research*, vol. 26, no. 2, pp. 138–142, 2003.

[30] G. Wang, Q. Cui, L.-J. Yin et al., "Efficient extraction of flavonoids from Flos Sophorae Immaturus by tailored and sustainable deep eutectic solvent as green extraction media," *Journal of Pharmaceutical and Biomedical Analysis*, vol. 170, pp. 285–294, 2019.

[31] Q. Yin, P. Wang, A. Zhang, H. Sun, X. Wu, and X. Wang, "Ultra-performance LC-ESI/quadrupole-TOF MS for rapid analysis of chemical constituents of Shaoyao-Gancao decoction," *Journal of Separation Science*, vol. 36, no. 7, pp. 1238–1246, 2013.

[32] C. Schmid, C. Dawid, V. Peters, and T. Hofmann, "Saponins from European licorice roots (Glycyrrhiza glabra)," *Journal of Natural Products*, vol. 81, no. 8, pp. 1734–1744, 2018.

[33] M. A. Farag, A. Porzel, and L. A. Wessjohann, "Comparative metabolite profiling and fingerprinting of medicinal licorice roots using a multiplex approach of GC-MS, LC-MS and 1D NMR techniques," *Phytochemistry*, vol. 76, pp. 60–72, 2012.

[34] T. Xu, M. Yang, Y. Li et al., "An integrated exact mass spectrometric strategy for comprehensive and rapid characterization of phenolic compounds in licorice," *Rapid Communications in Mass Spectrometry*, vol. 27, no. 21, pp. 2297–2309, 2013.

[35] L. Shan, N. Yang, Y. Zhao, X. Sheng, S. Yang, and Y. Li, "A rapid classification and identification method applied to the analysis of glycosides in Bupleuri radix and liquorice by ultra high performance liquid chromatography coupled with quadrupole time-of-flight mass spectrometry," *Journal of Separation Science*, vol. 41, no. 19, pp. 3791–3805, 2018.

[36] W. Song, X. Qiao, K. Chen et al., "Biosynthesis-based quantitative analysis of 151 secondary metabolites of licorice to differentiate medicinal Glycyrrhiza species and their hybrids," *Analytical Chemistry*, vol. 89, no. 5, pp. 3146–3153, 2017.

[37] Z. Li, T. Liu, J. Liao, N. Ai, X. Fan, and Y. Cheng, "Deciphering chemical interactions between Glycyrrhizae Radix and Coptidis Rhizoma by liquid chromatography with transformed multiple reaction monitoring mass spectrometry," *Journal of Separation Science*, vol. 40, no. 6, pp. 1254–1265, 2017.

[38] S. Fang, Q. Qu, Y. Zheng et al., "Structural characterization and identification of flavonoid aglycones in threeGlycyrrhizaspecies by liquid chromatography with photodiode array detection and quadrupole time-of-flight mass spectrometry," *Journal of Separation Science*, vol. 39, no. 11, pp. 2068–2078, 2016.

[39] S.-L. Li, H. Tan, Y.-M. Shen, K. Kawazoe, and X.-J. Hao, "A pair of new C-21 steroidal glycoside epimers from the roots of Cynanchum paniculatum," *Journal of Natural Products*, vol. 67, no. 1, pp. 82–84, 2004.

[40] X. Wang, X. Chen, J. Li et al., "Thrombin-based discovery strategy of bioactive-chemical quality marker combination for pollen of Typha orientalis by metabolomics coupled with chemometrics," *Phytomedicine*, vol. 75, Article ID 153246, 2020.

[41] M. Ding, Y. Jiang, X. Yu et al., "Screening of combinatorial quality markers for natural products by metabolomics coupled with chemometrics. A case study on pollen Typhae," *Frontiers in Pharmacology*, vol. 9, p. 691, 2018.

[42] D. Y. Lee, H. Yang, H. W. Kim, and S. H. Sung, "New polyhydroxytriterpenoid derivatives from fruits of Terminalia chebula Retz. and their α-glucosidase and α-amylase inhibitory activity," *Bioorganic & Medicinal Chemistry Letters*, vol. 27, no. 1, pp. 34–39, 2017.

[43] S. Sarabhai, P. Sharma, and N. Capalash, "Ellagic acid derivatives from Terminalia chebula Retz. downregulate the expression of quorum sensing genes to attenuate *Pseudomonas aeruginosa* PAO1 virulence," *Plos One*, vol. 8, no. 1, Article ID e53441, 2013.

[44] B. Pfundstein, S. K. El Desouky, W. E. Hull, R. Haubner, G. Erben, and R. W. Owen, "Polyphenolic compounds in the fruits of Egyptian medicinal plants (Terminalia bellerica, Terminalia chebula and Terminalia horrida): characterization, quantitation and determination of antioxidant capacities," *Phytochemistry*, vol. 71, no. 10, pp. 1132–1148, 2010.

[45] N. M. Fahmy, E. Al-Sayed, M. M. Abdel-Daim, M. Karonen, and A. N. Singab, "Protective effect ofTerminalia muelleriagainst carbon tetrachloride-induced hepato and nephrotoxicity in mice and characterization of its bioactive constituents," *Pharmaceutical Biology*, vol. 54, no. 2, pp. 303–313, 2016.

[46] K. Li, X. Han, R. Li et al., "Composition, antivirulence activity, and active property distribution of the fruit ofTerminalia chebulaRetz," *Journal of Food Science*, vol. 84, no. 7, pp. 1721–1729, 2019.

[47] F. Pellati, R. Bruni, D. Righi et al., "Metabolite profiling of polyphenols in a Terminalia chebula Retzius ayurvedic decoction and evaluation of its chemopreventive activity," *Journal of Ethnopharmacology*, vol. 147, no. 2, pp. 277–285, 2013.

[48] D. Y. Lee, H. W. Kim, H. Yang, and S. H. Sung, "Hydrolyzable tannins from the fruits of Terminalia chebula Retz and their α-glucosidase inhibitory activities," *Phytochemistry*, vol. 137, pp. 109–116, 2017.

[49] X. Sun, X.-B. Cui, H.-M. Wen et al., "Influence of sulfur fumigation on the chemical profiles of Atractylodes macrocephala Koidz. evaluated by UFLC-QTOF-MS combined with multivariate statistical analysis," *Journal of Pharmaceutical and Biomedical Analysis*, vol. 141, pp. 19–31, 2017.

[50] L. Lin, Q. Yang, K. Zhao, and M. Zhao, "Identification of the free phenolic profile of Adlay bran by UPLC-TOF-MS/MS and inhibitory mechanisms of phenolic acids against xanthine oxidase," *Food Chemistry*, vol. 253, pp. 108–118, 2018.

[51] A. Zhang, D. Zou, G. Yan, Y. Tan, H. Sun, and X. Wang, "Identification and characterization of the chemical constituents of Simiao Wan by ultra high performance liquid chromatography with mass spectrometry coupled to an automated multiple data processing method," *Journal of Separation Science*, vol. 37, no. 14, pp. 1742–1747, 2014.

[52] J.-J. Lu, X.-W. Hu, P. Li, and J. Chen, "Global identification of chemical constituents and rat metabolites of Si-Miao-Wan by liquid chromatography-electrospray ionization/quadrupole time-of-flight mass spectrometry," *Chinese Journal of Natural Medicines*, vol. 15, no. 7, pp. 550–560, 2017.

[53] S. Y. Kim, C. W. Choi, S. S. Hong, H. Shin, and J. S. Oh, "A New Neolignan from Coix lachryma-jobi var. mayuen," *Natural product communications*, vol. 11, no. 2, pp. 229–231, 2016.

[54] M. E. R. Andrade, R. D. G. C. D. Santos, A. D. N. Soares et al., "Pretreatment and treatment WithL-arginine attenuate weight loss and bacterial translocation in dextran sulfate sodium colitis," *Journal of Parenteral and Enteral Nutrition*, vol. 40, no. 8, pp. 1131–1139, 2016.

[55] W. Ren, J. Yin, M. Wu et al., "Serum amino acids profile and the beneficial effects of L-arginine or L-glutamine supplementation in dextran sulfate sodium colitis," *Plos One*, vol. 9, no. 2, Article ID e88335, 2014.

[56] L. A. Coburn, X. Gong, K. Singh et al., "L-arginine supplementation improves responses to injury and inflammation in dextran sulfate sodium colitis," *Plos One*, vol. 7, no. 3, Article ID e33546, 2012.

[57] H. Omidi-Ardali, Z. Lorigooini, A. Soltani, S. Balali-Dehkordi, and H. Amini-Khoei, "Inflammatory responses bridge comorbid cardiac disorder in experimental model of IBD induced by DSS: protective effect of the trigonelline," *Inflammopharmacology*, vol. 27, no. 6, pp. 1265–1273, 2019.

[58] J. Jin, Y. Zhong, J. Long et al., "Ginsenoside Rg1 relieves experimental colitis by regulating balanced differentiation of Tfh/Treg cells," *International Immunopharmacology*, vol. 100, Article ID 108133, 2021.

[59] Y. H. Choi, J.-K. Bae, H.-S. Chae et al., "Isoliquiritigenin ameliorates dextran sulfate sodium-induced colitis through the inhibition of MAPK pathway," *International Immunopharmacology*, vol. 31, pp. 223–232, 2016.

[60] X.-L. Yang, T.-K. Guo, Y.-H. Wang, M.-T. Gao, H. Qin, and Y.-J. Wu, "Therapeutic effect of ginsenoside Rd in rats with TNBS-induced recurrent ulcerative colitis," *Archives of Pharmacal Research*, vol. 35, no. 7, pp. 1231–1239, 2012.

[61] N. Yang, G. Liang, J. Lin et al., "Ginsenoside Rd therapy improves histological and functional recovery in a rat model of inflammatory bowel disease," *Phytotherapy Research*, vol. 34, no. 11, pp. 3019–3028, 2020.

[62] X.-r. Wang, H.-g. Hao, and L. Chu, "Glycyrrhizin inhibits LPS-induced inflammatory mediator production in endometrial epithelial cells," *Microbial Pathogenesis*, vol. 109, pp. 110–113, 2017.

[63] H. Ali, B. Weigmann, E.-M. Collnot, S. A. Khan, M. Windbergs, and C.-M. Lehr, "Budesonide loaded PLGA nanoparticles for targeting the inflamed intestinal mucosa-pharmaceutical characterization and fluorescence imaging," *Pharmaceutical Research*, vol. 33, no. 5, pp. 1085–1092, 2016.

[64] M. Zeeshan, H. Ali, S. Khan, M. Mukhtar, M. I. Khan, and M. Arshad, "Glycyrrhizic acid-loaded pH-sensitive poly-(lactic-co-glycolic acid) nanoparticles for the amelioration of inflammatory bowel disease," *Nanomedicine*, vol. 14, no. 15, pp. 1945–1969, 2019.

[65] X. Mao, R. Sun, Q. Wang et al., "l-Isoleucine administration alleviates DSS-induced colitis by regulating TLR4/MyD88/NF-kappaB pathway in rats," *Frontiers in Immunology*, vol. 12, Article ID 817583, 2021.

[66] M. K. Jeengar, D. Thummuri, M. Magnusson, V. G. M. Naidu, and S. Uppugunduri, "Uridine ameliorates dextran sulfate sodium (DSS)-Induced colitis in mice," *Scientific Reports*, vol. 7, no. 1, p. 3924, 2017.

[67] M. G. Zizzo, G. Caldara, A. Bellanca, D. Nuzzo, M. Di Carlo, and R. Serio, "Preventive effects of guanosine on intestinal inflammation in 2, 4-dinitrobenzene sulfonic acid (DNBS)-induced colitis in rats," *Inflammopharmacology*, vol. 27, no. 2, pp. 349–359, 2019.

[68] L. Zhu, P. Gu, and H. Shen, "Gallic acid improved inflammation via NF-κB pathway in TNBS-induced ulcerative colitis," *International Immunopharmacology*, vol. 67, pp. 129–137, 2019.

[69] A. K. Pandurangan, N. Mohebali, N. MohdEsa, C. Y. Looi, S. Ismail, and Z. Saadatdoust, "Gallic acid suppresses inflammation in dextran sodium sulfate-induced colitis in mice: possible mechanisms," *International Immunopharmacology*, vol. 28, no. 2, pp. 1034–1043, 2015.

[70] C. Mascaraque, C. Aranda, B. Ocón et al., "Rutin has intestinal antiinflammatory effects in the CD4+ CD62L+ T cell transfer

model of colitis," *Pharmacological Research*, vol. 90, pp. 48–57, 2014.

[71] H. Kim, H. Kong, B. Choi et al., "Metabolic and pharmacological properties of rutin, a dietary quercetin glycoside, for treatment of inflammatory bowel disease," *Pharmaceutical Research*, vol. 22, no. 9, pp. 1499–1509, 2005.

[72] S.-J. Kim, M.-C. Kim, J.-Y. Um, and S.-H. Hong, "The beneficial effect of vanillic acid on ulcerative colitis," *Molecules*, vol. 15, no. 10, pp. 7208–7217, 2010.

[73] Y. Bian, P. Liu, J. Zhong et al., "Quercetin attenuates adhesion molecule expression in intestinal microvascular endothelial cells by modulating multiple pathways," *Digestive Diseases and Sciences*, vol. 63, no. 12, pp. 3297–3304, 2018.

[74] Y. Dong, J. Lei, and B. Zhang, "Dietary quercetin alleviated DSS-induced colitis in mice through several possible pathways by transcriptome analysis," *Current Pharmaceutical Biotechnology*, vol. 21, no. 15, pp. 1666–1673, 2020.

[75] J. Zhang, L. Cao, H. Wang et al., "Ginsenosides regulate PXR/NF-κB signaling and attenuate dextran sulfate sodium-induced colitis," *Drug Metabolism and Disposition*, vol. 43, no. 8, pp. 1181–1189, 2015.

[76] M. El-Sherbiny, N. H. Eisa, N. F. Abo El-Magd, N. M. Elsherbiny, E. Said, and A. E. Khodir, "Anti-inflammatory/anti-apoptotic impact of betulin attenuates experimentally induced ulcerative colitis: an insight into TLR4/NF-kB/caspase signalling modulation," *Environmental Toxicology and Pharmacology*, vol. 88, Article ID 103750, 2021.

[77] Q. He, L. He, F. Zhang et al., "Stachyose modulates gut microbiota and alleviates dextran sulfate sodium-induced acute colitis in mice," *Saudi Journal of Gastroenterology*, vol. 26, no. 3, pp. 153–159, 2020.

[78] C. Cheng, W. Zhang, C. Zhang et al., "Hyperoside ameliorates DSS-induced colitis through MKRN1-mediated regulation of PPARγ signaling and Th17/treg balance," *Journal of Agricultural and Food Chemistry*, vol. 69, no. 50, pp. 15240–15251, 2021.